International Journal of Environmental Science and Technology
https://doi.org/10.1007/s13762-024-05814-2

ORIGINAL PAPER

# Study of caesium adsorption onto alluvial sediments from the Italian Po Plain

F. Giacobbo[1] · F. Pezzoli[1] · I. Cydzik[2] · M. Da Ros[1] · M. Dapiaggi[3] · M. Giudici[3]

Received: 6 November 2023 / Revised: 28 May 2024 / Accepted: 4 June 2024


## Abstract

The study investigates the adsorption processes of caesium onto alluvial sediments from the Po Plain (northern Italy). Understanding these adsorption processes is crucial for assessing the safety of low- and intermediate-level radioactive waste repositories, including the proposed Italian repository. Adsorption kinetics and equilibrium experiments on sandy samples were conducted with the aim of evaluating how even small differences in clay content and mineralogy can affect kinetics and equilibrium adsorption behaviour. The obtained data were compared with literature studies and confirmed the significant affinity of caesium for sandy sediments, even for a mud content of less than 5%. Kinetics analysis revealed that a pseudo-second-order model best described the process, suggesting two-site occupancy adsorption kinetics attributed to the presence of illite and characterised by various different sites for caesium adsorption. Samples with higher clay and micaceous minerals content, cation exchange capacity and specific surface area exhibit faster kinetics and higher affinity for caesium. The study shows a significant variation in partition coefficient values, ranging from 57 to 750 mg $L^{-1}$. This finding emphasises the importance of sediment composition in caesium adsorption, which is crucial for developing accurate environmental protection and safety assessment models.

**Keywords** Adsorption · Batch test · Caesium · Isotherm model · Kinetic test · Sandy sediments · Clay

## Introduction

Among the radioisotopes found in low- and intermediate-level radioactive wastes (LLW and ILW, respectively), $^{137}Cs$ is one of the most relevant. It is a fission product commonly found in nuclear reactor waste or spent nuclear fuel waste from reprocessing plants (Lee et al. 2013). Radioactive isotopes of caesium, $^{137}Cs$ and $^{134}Cs$, were also released into the environment with the fallout from accidental releases, such as the Chernobyl and Fukushima accidents (Yasunari et al. 2011; Nakanishi et al. 2013; Steinhauser et al. 2014; Okumura et al. 2019; Tachi et al. 2020), and from tests of nuclear weapons.

The solubility in water of halides with caesium as the electropositive element is quite high; therefore, caesium can be easily dissolved in water (Greenwood and Earnshaw 1997; Ueda et al. 2012). Therefore, once released into the environment, caesium can be dispersed by groundwater flow. Moreover, due to the half-life of radiocaesium and its capability to be assimilated by living organisms (Zhu and Smolders. 2000; Nakanishi et al. 2013), caesium can be harmful to human health. If inhaled or ingested, caesium can accumulate in vital organs, and its beta and high-energy gamma emissions can induce the formation of tumours (Endo 2012; Steinhauser et al. 2014).

On the basis of the above remarks, it is clear that numerical predictive models which simulate solute transport in geological porous media and which are often used in safety assessment studies of radioactive waste repositories (Lee et al. 2013) should consider the behaviour of radiocaesium in the environment. Accurate modelling and reliable predictions require knowledge of the hydrogeological properties of the involved geological formations

Editorial responsibility:S. Mirkia.

✉ F. Giacobbo
francesca.giacobbo@polimi.it

[1] Dipartimento di Energia, Politecnico di Milano, Piazza Leonardo da Vinci 32, 20133 Milan, MI, Italy

[2] Nucleco S.p.a., Via Anguillarese, 301, 00123 Roma, Italy

[3] Dipartimento di Scienze della Terra "A. Desio", Università degli Studi di Milano, Via Botticelli 23, 20133 Milan, MI, Italy

Published online: 19 June 2024

and the adsorption processes that govern the exchanging phenomena between liquid and solid phases.

In this regard, to model the extent and the rate at which caesium ions are removed from aqueous solutions through adsorption on the solid matrix, it is important to study and model adsorption processes and their kinetics at the laboratory scale. Therefore, the experimental study of adsorption processes of caesium ions onto underground porous media and onto porous matrices suitable for remediation and water decontamination purposes is a key point for environmental protection and cleanup as well as for safety assessment of nuclear waste repositories (Bouzidi et al. 2010; Caccin et al. 2013; Lee et al. 2013; Ding et al. 2016; Lemieux et al. 2018; Szabo 2018; Gouda et al. 2019; Park et al. 2019; Tachi et al. 2020).

Adsorption of caesium on pure minerals and on heterogeneous media has been extensively studied (Torstenfelt et al. 1982; Sheppard and Thibault 1990; Cornell 1993; Staunton and Roubaud 1997; Wang et al. 2010; Tsuji et al. 2014). Such studies showed that caesium is mainly adsorbed through charge-compensating cation exchange onto the finest fraction of clay minerals, which are characterised by a high cation exchange capacity (CEC), a large specific surface area and a high density of available charged surface sites together with interlayer and interlayer-edge sites (Cornell 1993; Meunier 2005; Giannakopoulou et al. 2007; Fuller et al. 2014; Lee et al. 2017).

The minerals of interest for caesium adsorption are principally clay and mica, including illite, smectite, kaolinite, muscovite, vermiculite and biotite. Indeed, clay and micaceous minerals behave selectively towards cations which have low hydration energy, like caesium, and which are mainly adsorbed through ion exchange with cations present in the mineral interlayers or through interaction with the hydroxyl and oxide groups present on the surface. For instance, in the case of illite, caesium adsorption is interpreted with multi-site ion exchange models due to the presence of various adsorption sites. Among these sites, the frayed edge sites (FES) play an important role in caesium uptake due to their high selectivity for caesium also in trace concentrations (Comans et al. 1991; Cornell 1993; Mc Kinley et al. 2004; Giannakopoulou et al. 2007; Benedicto et al. 2014; Missana et al. 2014a; Fuller et al. 2015; Cherif et al. 2017; Lee et al. 2017; Yin et al. 2017; Durrant et al. 2018; Ferreira et al. 2018; Okumura et al. 2019; Park et al. 2019, 2021; Hwang et al. 2021; Li et al. 2021; Latrille and Bildstein 2022; Zhang et al. 2022).

Therefore, the clay content of the porous matrix can be considered one of the main factors that affect caesium adsorption, together with the CEC of the solid matrix, the pH and ionic strength of the solution and the presence of competing ions in solution (Shenber and Eriksson 1993; Flury et al. 2004; Giannakopoulou et al. 2007; Missana et al. 2014b; Testoni et al. 2017; Semenkova et al. 2018).

Due to the above-mentioned factors, the development of accurate models of caesium ion transport by groundwater is quite challenging and requires site-specific studies of adsorption processes, both under static and dynamic conditions.

To examine this issue, this work studies caesium adsorption onto alluvial sediments from the Po Plain (Italy) under static conditions at the laboratory scale. The sampled sediments can be considered representative of sediments that are present in most of the potential sites for the foreseen Italian nuclear waste repository, which have been selected by Sogin S.p.A., the state-owned company in charge of the nuclear waste management on the Italian territory (CNAPI 2020).

Three sandy samples were collected and used for this work. Despite being representative of very similar lithological and geological units, they showed some small differences in the content and mineralogy of clays. Therefore, they are expected to be very useful in evaluating the influence of the clay content and mineralogy on caesium adsorption on sandy sediments.

Within this framework, the general objective of this work is to assess if small differences in clay content and mineralogy among sandy samples can have effects that are appreciable with laboratory tests. Furthermore, the goal is to assess if small variations among the samples could yield experimental data, which should be fitted with different phenomenological models. In other words, this work is expected to provide further qualitative and possibly quantitative insights into the effects that clay minerals have on caesium adsorption on sandy sediments.

This objective is pursued through kinetic and equilibrium batch tests for six different associations of sandy samples and aqueous solutions containing caesium ions. Aqueous solutions containing dissolved caesium are created using two commercial mineral waters. The kinetic and equilibrium batch results and their fit by kinetic and isotherm models are compared with results from similar literature studies.

The paper is organised as follows: the 'Material and Methods' section describes the studied sediment samples from the adopted waters and reagents and the applied adsorption test procedure; the 'Results and Comparison with Literature' section reports the results of kinetic and batch experiments, their interpretation with respect to kinetic and isotherm equilibrium models and a comparison with literature studies regarding similar matrices; and 'Conclusion' section ends the paper.

## Materials and methods

### Samples

Sandy sediments used in this work derive from soil pits excavated in the Po Plain (northern Italy; Inzoli 2016). Samples were taken from outcrops of sediments at Orio Litta and

Senna Lodigiana. In the following, samples are indicated as SA10-A1, SA11-A4 and OA2-A1, where the acronym SA stands for Senna Lodigiana, and OA for Orio Litta, while letters and numbers refer to internal laboratory classification (Inzoli 2016). For details regarding the sampling area, refer to the Supplementary Material.

Results of grain size analysis, carried out with sieve analysis (Inzoli 2016), are listed in Table 1 in terms of percentages of gravel, sand and mud according to Wentworth's classification. The fraction of mud was obtained by summing the silt and clay fractions. Samples are characterised by their variable sandy texture. Samples SA10-A1 and OA2-A1 were predominantly medium sand, sample SA11-A4 was coarse sand, and sample OA2-A1 contained the largest percentage of mud.

The composition of the samples was quantitatively determined using X-ray powder diffraction analysis (XRD) with a PANalytical X'Pert PRO diffractometer and the Rietveld method, using the software Gsas2 (Toby and Von Dreele 2013). Total CEC was determined using the barium chloride method. The CEC of Na, K, Mg and Ca was measured (Ciesielski et al. 1997) with an inductively coupled plasma mass spectrometer (ICP-MS Agilent 7700). The specific surface area of the samples was determined using

**Table 1** Grain size distribution according to Wentworth's classification; composition; cation exchange capacity (CEC) values; specific surface area

| Sample | SA10-A1 [wt%] | SA11-A4 [wt%] | OA2-A1 [wt%] |
|---|---|---|---|
| *Grain size distribution* | | | |
| Mud (silt and clay) | 3.47 | 1.6 | 5.18 |
| Sand | 96.42 | 98.4 | 92.1 |
| *vfS* | 0.65 | 0 | 1.5 |
| *fS* | 31.17 | 0.18 | 8.9 |
| *mS* | 53.09 | 31.42 | 60.2 |
| *cS* | 9.26 | 59.29 | 19.9 |
| *vcS* | 2.25 | 7.51 | 1.6 |
| Granules | 0.11 | 0 | 0.94 |
| Pebbles | 0 | 0 | 1.78 |

| | | SA10-A1 | SA11-A4 | OA2-A1 |
|---|---|---|---|---|
| *Composition* | | | | |
| Quartz [wt%] | Qz | 14.5 | 33.3 | 18.6 |
| Calcite [wt%] | Cal | 4.5 | - | 5.2 |
| Dolomite [wt%] | Dol | 64.0 | 3.1 | 47.7 |
| Mica (illite) [wt%] | M | 3.7 | 16.5 | 6.0 |
| Chlorite [wt%] | Chl | 5.2 | 6.5 | 11.3 |
| Albite [wt%] | Ab | 8.1 | 24.2 | 10.1 |
| Orthoclase [wt%] | Or | – | 6.4 | 1.2 |
| Amphibole [wt%] | Amp | – | 2.9 | – |
| Vermiculite [wt%] | Vrm | – | 7.1 | – |
| | | Error < 0.2 wt% | | |
| *Cation Exchange Capacity [c mol$^+$ kg soil$^{-1}$]* | | | | |
| CEC | | 4.37 ± 0.1 | 6.67 ± 0.42 | 4.80 ± 0.06 |
| $Na^+$ | | 0.93 ± 0.01 | 1.06 ± 0.01 | 0.85 ± 0.01 |
| $K^+$ | | 0.18 ± 0.02 | 0.18 ± 0.02 | 0.15 ± 0.02 |
| $Ca^{2+}$ | | 5.23 ± 0.01 | 5.38 ± 0.01 | 4.54 ± 0.01 |
| $Mg^{2+}$ | | 0.27 ± 0.02 | 0.50 ± 0.02 | 0.19 ± 0.02 |
| *BET analysis* | | | | |
| Specific surface area [$m^2g^{-1}$] | | 1.822 ± 0.011 | 2.597 ± 0.019 | 1.267 ± 0.008 |

Wentworth's classification

Particles larger than 64 mm in diameter are classified as cobbles, while smaller particles are pebbles, granules, sand and silt. The sandy fraction (grain diameter between 63 µm and 2 mm) is further distinguished into five sub-classes: very coarse (vc), coarse (c), medium (m), fine (f) and very fine (vf) sand. Silt includes particles with a diameter between 4 µm and 63 µm, while those smaller than 4 µm are clay; mud includes silt and clay

Brunauer–Emmet–Teller (BET) analysis (ISO 2022) with Micromeritics® TriStar II 3020. Results are reported in Table 1. The quantity of organic matter content was lower than 0.4 wt%.

All the samples showed the presence of quartz and dolomite, with some differences. In SA10-A1, quartz and dolomite are the dominant mineral phases, forming almost 80% of the total material. The remaining mineral phases are approximately uniformly distributed among calcite, feldspar (albite), illite and chlorite.

In SA11-A4, quartz, mica (illite) and chlorite cover almost 60% of the whole sample. The quantity of dolomite is small, feldspars (albite and orthoclase) are more abundant than in the other two samples, vermiculite and some amphibole can be found. No calcite is found in this sample.

In OA2-A1, quartz and dolomite are predominant: together they form almost 70% of the whole material. The remaining fraction is approximately uniformly distributed among chlorite, feldspars (albite and orthoclase), mica (illite) and calcite.

The major differences among the samples appear to be the abundance of dolomite, which decreases from OA2-A1 to SA10-A1 and is significantly lower in SA11-A4, and the relatively high amount of clay and micaceous minerals in the mud component of SA11-A4 sample.

Among minerals like smectite, vermiculite, montmorillonite and zeolites, for which caesium adsorption affinity has been extensively studied (Staunton and Roubaud 1997; Missana et al. 2014a; Tsuji et al. 2014; Fuller et al. 2015; Durrant et al. 2018; Ferreira et al. 2018; Hwang et al. 2021; Latrille and Bildstein 2022), vermiculite is only present in the finest fraction ($d < 2$ μm) of SA11-A4.

## Water

As suggested by the American Society for Testing and Materials (ASTM) guidelines (ASTM 2021), adsorption studies on natural sediments should be ideally performed with aqueous solutions prepared with groundwater sampled at the study sites. This procedure was impractical for the case under study; therefore, a different procedure was chosen for the selection of the two waters adopted for this study. For the sake of brevity, the procedure is reported in the Supplementary Material.

Table 2 compares the chemical compositions of the drinking water of the sampling areas with those of two selected commercial mineral waters, which differ from each other in the content of dissolved electrolytes. Water V is the one that best simulates the composition of the drinking water of the Senna Lodigiana area in terms of the content of dissolved electrolytes and pH among all the considered mineral waters. Water A has been chosen for its very low content of dissolved electrolytes in order to possibly highlight different adsorption behaviours dependent on dissolved electrolyte content. Both waters have pH value inside the typical range of groundwaters (i.e., pH from 5 to 9; Cornell 1993).

The main cations analysed during the laboratory experiments were calcium, sodium, magnesium, strontium and potassium. Anions that are present, sometimes in traces, in the Senna Lodigiana and Orio Litta waters as well as in waters A and V are $HCO_3^-$, $SO_4^{2-}$, $Cl^-$, $NO_3^-$ and $F^-$. Indeed, the presence in groundwater of complexing anions can lead to the formation of complexing compounds with contaminant ions in solution, resulting in a lower potential for adsorption and increasing their solubility. Nevertheless, because caesium ions in soil/water environments have very little tendency to form aqueous complexes, the effect that anions in solution could have on adsorption phenomena has been considered negligible (Carbol and Engkvist 1997; EPA 1999).

## Reagents

Appropriate stock solutions were prepared by dissolving chloride salt, CsCl, in the selected commercial waters with initial concentrations varying from 0.25 to 30 mg $L^{-1}$. Since caesium chloride is characterised by high solubility, a large availability of dissociated caesium ions in solution should be ensured. Moreover, a chloride salt containing $^{133}Cs$ stable isotope was used (Yoshida et al. 2004; Giannakopoulou et al. 2007). All chemicals and reagents used were of analytical reagent (AR) grade. The absence of caesium adsorption onto the flasks, filters and adopted materials was checked. Experiments were conducted in isothermal conditions at ambient temperature (i.e., 22 ℃).

**Table 2** Total dissolved solids [mg $L^{-1}$], pH and concentration [mg $L^{-1}$] of main cations of the waters of Senna Lodigiana and Orio Litta areas and of the two commercial waters V and A

| | Drinking water Senna Lodigiana | Drinking water Orio Litta | Water V | Water A |
|---|---|---|---|---|
| Total dissolved solids | 441 | 241 | 382 | 39 |
| $Ca^{2+}$ | 111 | 63 | 88.7 | 4.4 |
| $Na^+$ | 15 | 14 | 4.3 | 2.6 |
| $Mg^{2+}$ | 27 | 14 | 34.8 | 0.6 |
| $K^+$ | 3 | 2 | 5.6 | 4.4 |
| pH | 8.0 | 8.1 | 8.0 | 7.4 |

### Adsorption tests procedure

Caesium kinetic and equilibrium adsorption tests were carried out for six different associations of sandy samples and aqueous solutions. Particularly, the SA10-A1, SA11-A4 and OA2-A1 samples were kept in contact with aqueous solutions containing CsCl and prepared with the two selected waters, V and A.

Adsorption tests were performed according to the following procedure. In 50 mL Erlenmeyer flasks, containing 4 g of sediment sample in contact with 40 mL of an aqueous solution containing the prescribed initial concentration of CsCl, were kept on an orbital stirrer at a speed of 170 rpm for the required time intervals at controlled ambient temperature. The solid-to-liquid mass ratio of 1:10 was chosen in compliance with the literature (Giannakopoulou et al. 2007, 2012; Reynolds et al. 1982). After pre-fixed time intervals, the sediments were separated from the supernatant and filtered with 0.45 µm PES syringe filters. The residual concentration of the elements of interest (Cs, Na, Mg, K, Ca and Sr) in the sampled and filtered solution was measured by mass spectrometry. Thermo Fischer XSeries II, Bruker aurora M90 and Agilent 7700 ICP mass spectrometers were used for different sets of measures. Each sample was measured three or five times to get the concentration average value. The pH values of the filtered supernatant were also measured.

The amount of adsorbed mass was determined by the difference between the initial and the residual ion concentration in the aqueous solution. The concentration of sorbate on the solid phase at time t, $S_t$ [mg $g^{-1}$], was calculated according to the following formula:

$$S_t = \frac{(C_0 - C_t)V}{M} \quad (1)$$

where $C_0$ is the initial concentration of solute in the liquid phase [mg $L^{-1}$], $C_t$ is the residual concentration of solute in the liquid phase at time $t$ [mg $L^{-1}$], $M$ is the dry mass of the sediment sample [mg] and $V$ is the volume of the liquid phase [L]. When equilibrium is reached (i.e., after a sufficiently long time), the concentration in solution $C_t$ and the concentration of the adsorbed mass $S_t$ become constant and are denoted, respectively, as $C_e$ (i.e., the concentration in solution at equilibrium) and $S_e$ (i.e., the concentration of adsorbed mass at equilibrium).

Preliminary release tests were carried out to determine the possible release of caesium ions by the sediment samples. None of the three sediment samples in contact with ultrapure water and A and V waters released any detectable concentration of caesium ions after a reasonable time (see Supplementary Material for details).

Kinetic batch tests were carried out to estimate the equilibrium time for the six different associations of sediment sample/aqueous solution containing CsCl. For all the kinetic experiments, the initial concentration of CsCl was set equal to 5 mg $L^{-1}$.

After six contact times, in the interval between 2 and 329 h, aliquots of supernatant were filtered with 0.45 µm PES syringe filters. The contact times were selected by considering ASTM guidelines (ASTM 2021) and some published evidence regarding caesium adsorption rates onto sandy matrices (Cornell 1993). The pH of the solutions was measured for all the collected aliquots. Experiments have been designed to give a clear information about the adsorption trend as a function of time. Equilibrium times were estimated based on experimental data and by considering the trend of the experimental results and the amplitude of the error bars.

The used solvents were commercial mineral waters, so that other ions different from caesium may be present in solution. To study possible adsorption/desorption of Na, Mg, K, Ca and Sr ions by the sediment samples in contact with the commercial mineral waters, specific kinetic tests were performed, in absence and in presence of dissolved caesium (5 mg $L^{-1}$). Residual concentrations of Na, Mg, K, Ca and Sr were measured as a function of contact time, up to 329 h. The results of this analysis integrate the experimental data, but have modest relevance on the main conclusions of this work; therefore, they have only been included in the Supplementary Material.

Equilibrium batch tests to determine the equilibrium isotherm of Cs were performed for six different associations of sandy samples and aqueous solutions containing CsCl. The initial concentration varied from 0.25 to 30 mg $L^{-1}$. For tests with water A, the initial concentration of 0.01 mg $L^{-1}$ was also considered.

### Models

Experimental data were fitted with kinetic and equilibrium isotherm models (Weber and Morris 1963; Ho and McKay 1999; Rudzinski and Plazinski 2006; Foo and Hameed 2010; Malash and El-Khaiary 2010; Li et al. 2010; Caccin et al. 2016; Ayawei et al. 2017) and compared with data and models from the literature references (Reynolds et al. 1982; Toshiaki 1984; Sheppard and Thibault 1990; El-Reefy et al. 1994; Tanaka and Ohnuki 1994; Staunton and Roubaud 1997; Huitti et al. 2000; Shahwan and Erten 2002; Zachara et al. 2002; Flury et al. 2004; Giannakopoulou et al. 2007, 2012; Yildiz et al. 2011; Ugur and Sahan 2012; Hamed et al. 2016; Hassan 2016).

## Results and comparison with literature

### Kinetic test results

All three sandy samples show a high affinity for caesium; the percentage of adsorbed caesium is 92% of that initially

dissolved in solution. The pH of all the aliquots collected over time remained almost constant during the tests (i.e., about 7.4 for the tests with water A and about 8 for the tests with water V). Therefore, during the kinetic experiments, the pH values remained inside the typical range of groundwater (i.e., from 5 to 9; Cornell 1993). The estimated experimental equilibrium times $t_{e,exp}$ obtained from the kinetic tests for the six associations of the sediment samples and aqueous solutions are SA10-A1 170 h, SA11-A4 24 h and OA2-A1 120 h with water A and SA10-A1 240 h, SA11-A4 170 h and OA2-A1 240 h with water V. The associated equilibrium concentrations, $S_e$, attain values of around 0.046 mg $g^{-1}$. Results are reported in the Supplementary Material. The experimental kinetic results of caesium adsorption were fitted with pseudo-first-order and pseudo-second-order kinetic models (Ho and McKay 1999; Rudzinski and Plazinski 2006).

### Pseudo-first-order kinetic model

The pseudo-first-order kinetic Lagergren model, which is associated with a one-site occupancy adsorption kinetics, corresponds to the following equation:

$$\frac{dS_t}{dt} = K_1(S_e - S_t) \tag{2}$$

where $K_1$ [$h^{-1}$] is the Lagergren rate constant of first-order adsorption, $S_t$ is the mass of contaminant adsorbed per unit mass of sorbent matrix at time $t$ [mg $g^{-1}$] and $S_e$ is the mass of contaminant adsorbed per unit mass of sorbent matrix at equilibrium [mg $g^{-1}$].

By integrating (2) in time from 0 to $t$, and assuming $S_t$ (0) = 0 and $S_t$ (∞) = $S_e$, the following solution can be obtained:

$$S_t = S_e(1 - e^{-K_1 t}) \tag{3}$$

The fit of the experimental kinetic data with (3) is shown in Fig. 1. For the sake of brevity, the correspondent pseudo-first-order kinetic parameters are reported in the Supplementary Material.

### Pseudo-second-order kinetic model

The pseudo-second-order kinetic model, which is a generalisation of the pseudo-first-order model, describes two-sites-occupancy adsorption kinetics and corresponds to the following equation:

$$\frac{dS_t}{dt} = K_2\left(S_e - S_t\right)^2 \tag{4}$$

where $K_2$ is the rate constant of second-order adsorption [g $mg^{-1}$ $h^{-1}$].

By separating the variables and integrating in time from 0 to $t$ with the initial condition $S_t(0) = 0$, Eq. (4) yields the following:

$$\frac{t}{S_t} = \frac{t}{S_e} + \frac{1}{K_2 S_e^2} \tag{5}$$

The fit of experimental data is shown in Fig. 2. The corresponding pseudo-second-order kinetic parameters are reported in the Supplementary Material.

### Intra-particle diffusion model

To interpret the kinetics results, the empirical diffusion model of Weber and Morris was adopted by assuming a two-step diffusion process (Weber and Morris 1963). According to this model, the rates of diffusion can be calculated by linearising the following equation:

$$S_t = K_i t^{0.5} + C_i \tag{6}$$

where, $K_i$, $i$ = 1,2, are the kinetic constants relative to the $i$-th step of the adsorption process [mg (g $h^{0.5})^{-1}$], $C_i$ is the intercept of $i$-th step [mg $g^{-1}$], and $C_1$ = 0, because it is assumed that no caesium is initially adsorbed.

According to this model, the plot of adsorbed amount of ions, $S_t$, versus the square root of time, $t^{0.5}$, should be linear if diffusion is involved in the adsorption process.

The amount of experimental data in this study does not enable a robust estimate of the diffusion coefficients to be obtained, but it is nevertheless possible, as a first approximation, to examine the potential presence of a multi-linear trend due to a two-step diffusion process (Malash and El-Khaiary 2010). To this aim, kinetic data have been interpreted according to the intra-particle diffusion model of Eq. (6). Results are reported in Fig. 3.

Specific kinetic tests that lasted up to 329 h were used to check the concentrations of Na, Mg, K, Ca and Sr ions in solution in the commercial mineral waters A and V in contact with the three sediment samples and in the presence of Cs in solution. No relevant differences can be noticed between the two conditions, namely the presence or absence of dissolved caesium. Results can be found in the Supplementary Material.

## Batch test results

The relative errors of the measurements are generally lower than 3%. For some samples, the relative error on $C_e$ is of the order of 10% and the corresponding error on $S_e$ is estimated, with error propagation theory, to be smaller than 4%.

Analogously to kinetic tests, the pH values were almost constant for all the batch tests (i.e., about 7.4 for the tests with water A and about 8 for the tests with water V). Details

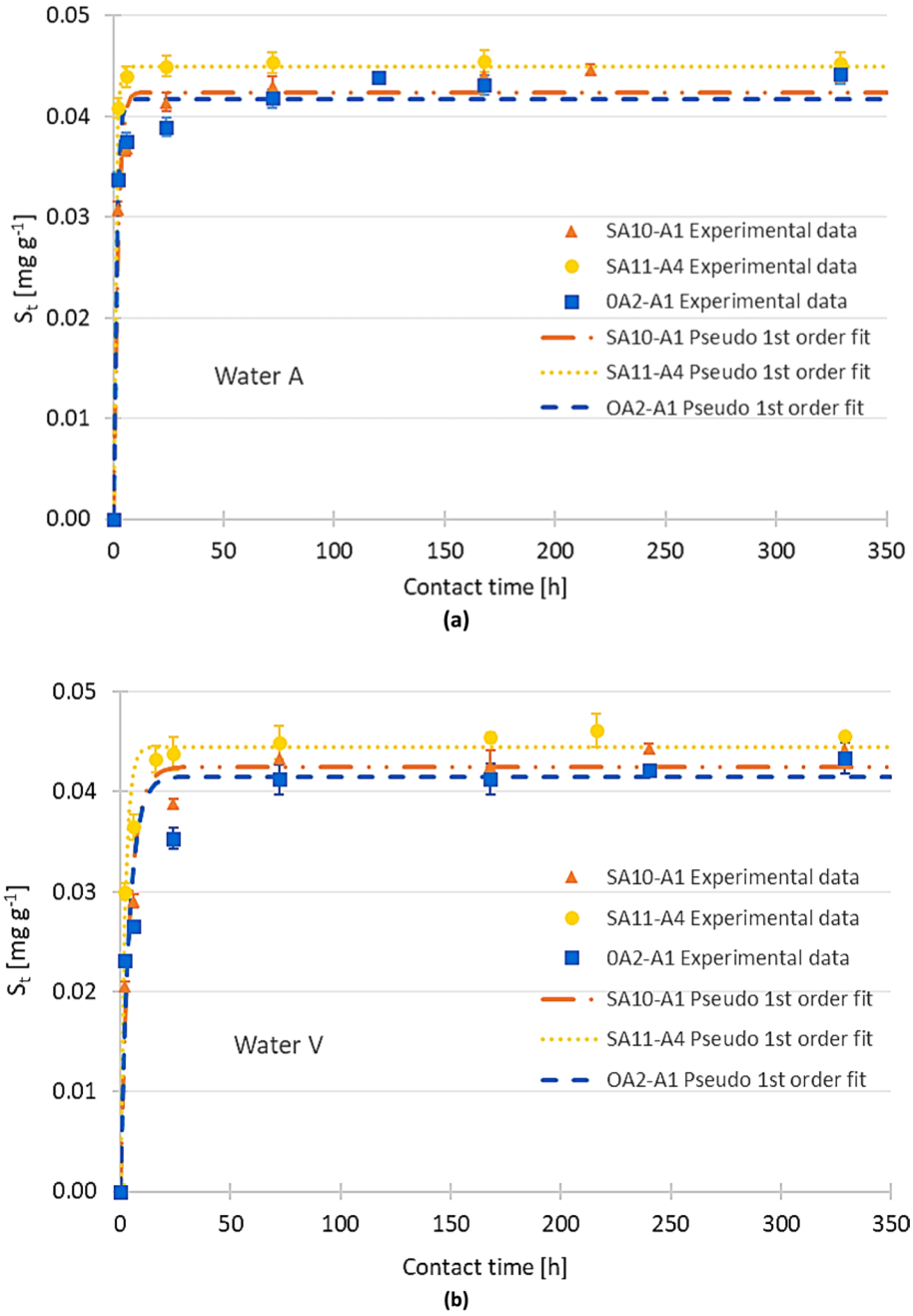


**Fig. 1** Pseudo-first-order adsorption kinetic models of caesium ions adsorption onto the sediment samples. Contact solution: **a** water A, **b** water V

regarding the experimental results obtained with the three different samples and the two aqueous solutions are reported in the Supplementary Material.

### Isotherm models

Experimental data were fitted with linear, Langmuir, Freundlich and Brunauer–Emmet–Teller models (Foo and Hameed 2010; Ayawei et al. 2017).

The equilibrium linear isotherm model, the most used for batch experimental data analysis, assumes a linear relationship between the concentration of solute in solution at equilibrium, $C_e$, and the corresponding mass of sorbate per unit mass of solid matrix, $S_e$:

$$S_e = K_d C_e \tag{7}$$

where $K_d$ is the linear distribution coefficient [mL g$^{-1}$].

The equilibrium Langmuir isotherm law corresponds to a theoretical model valid for mono-layer adsorption onto a surface with a finite number of equivalent sites, each of them having the same affinity towards the sorbate. The Langmuir equation is the most widely used two-parameter model and is commonly expressed as:

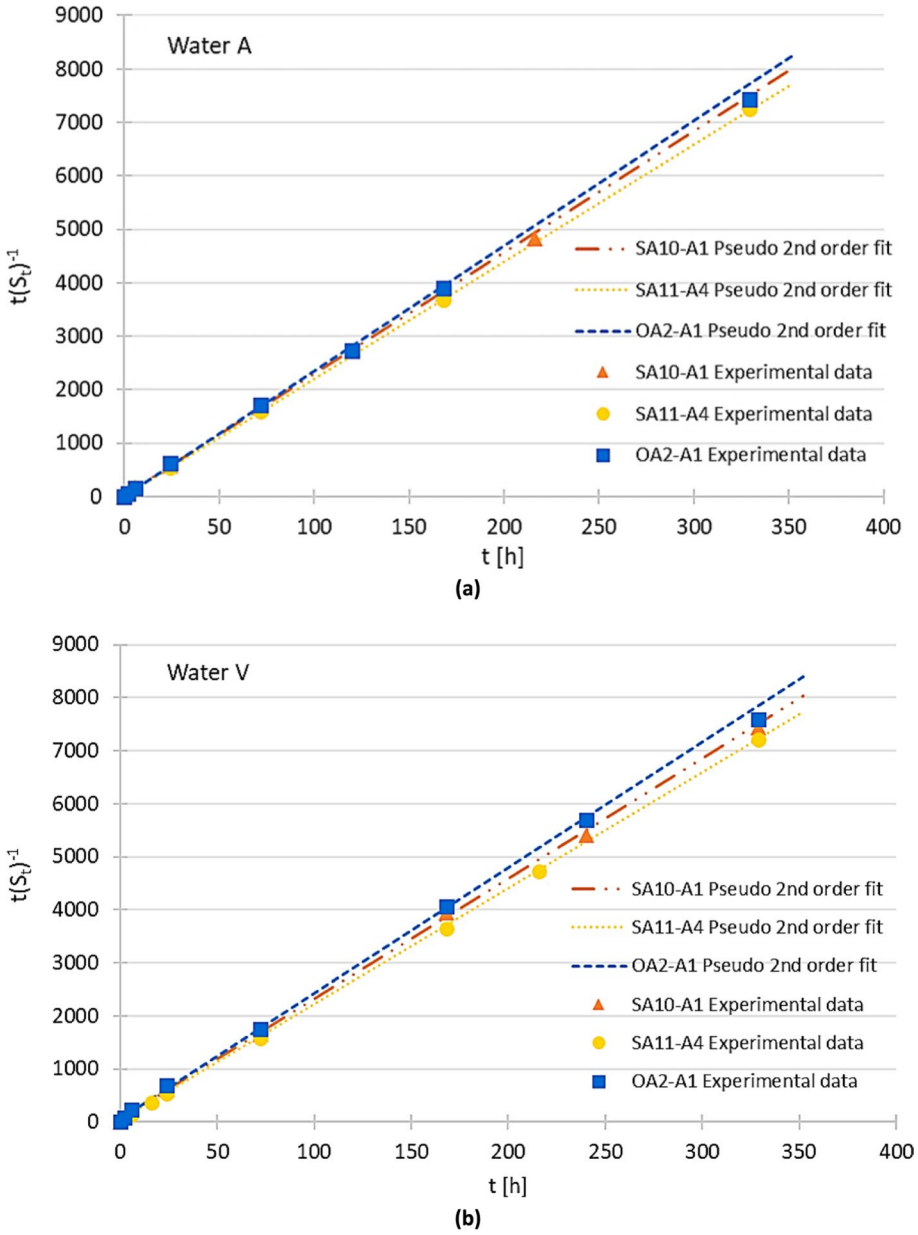


**Fig. 2** Pseudo-second-order adsorption kinetic models of caesium ions adsorption onto the sediment samples. Contact solution: **a** water A, **b** water V

$$S_e = \frac{S_{max} K_L C_e}{1 + K_L C_e} \tag{8}$$

where $K_L$ is the Langmuir adsorption coefficient related to the energy of adsorption [L mg$^{-1}$] and $S_{max}$ is the maximum adsorption capacity of the sorbent [mg g$^{-1}$]. The two coefficients can be determined from the slope and the intercept of the plot of $C_e/S_e$ versus $C_e$. In fact, to fit experimental data, Eq. (8) can be linearised as:

$$\frac{C_e}{S_e} = \frac{1}{S_{max} K_L} + \frac{C_e}{S_{max}} \tag{9}$$

which enables constants to be derived with linear regression.

The Freundlich isotherm is an empirical law and assumes a heterogeneous surface onto which multi-layer adsorption takes place. At equilibrium conditions, the adsorbed concentration can be described using the following equation:

$$S_e = K_F C_e^{\,1/n} \tag{10}$$

where $n$ is a positive constant and $K_F$ is the Freundlich adsorption coefficient (i.e., the sorbent capacity [(mg g$^{-1}$)•(mg L$^{-1}$)$^{-1/n}$]). The exponent $1/n$ is usually lower than 1 and decreases with surface heterogeneity; however, it may be greater than 1 when cooperative adsorption processes take place (Haghseresht and Lu 1998; Foo and Hameed 2010).

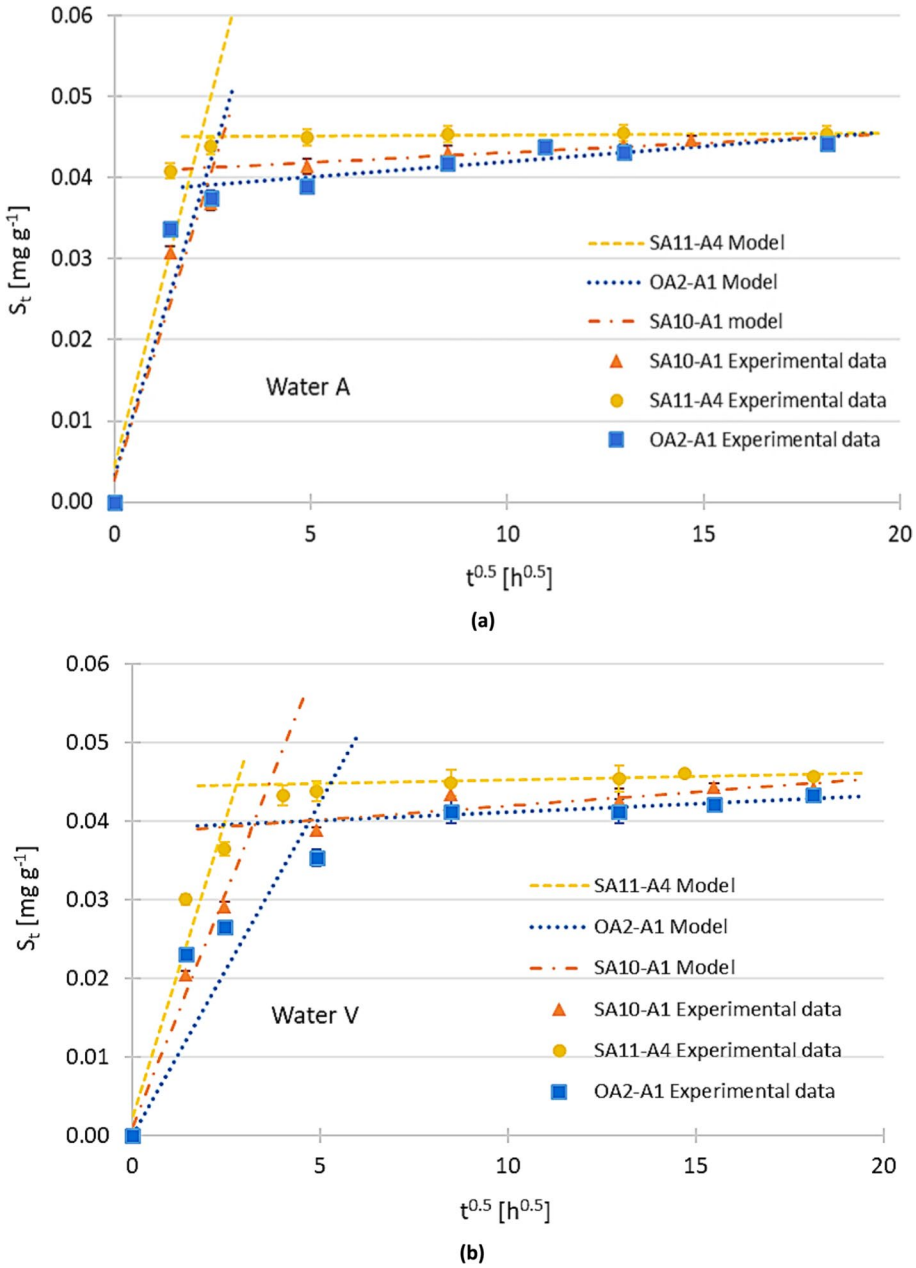


**Fig. 3** Adsorption kinetics of caesium onto the sediment samples: intra-particle diffusion model. Contact solution: **a** water A, **b** water V

For the linear regression of the experimental data, the linear form of Eq. (10) is the following:

$$log_{10}S_e = log_{10}K_F + \frac{1}{n}log_{10}C_e \tag{11}$$

The Brunauer-Emmet-Teller (BET) model is a three-parameter model, which is mostly applied to gas–solid systems and can also be adopted for liquid phase adsorption to describe multi-layer adsorption. However, the BET model can also be extended to liquid–solid systems such as the phenol-activated carbon systems (Ebadi et al. 2009; Girods et al. 2009). One of its applications is the determination of surface area/pore size distribution of a porous matrix. The BET isotherm model is the following:

$$S_e = \frac{S_m C_{BET} C_e}{\left(C_m - C_e\right)\left[1 + \left(C_{BET} - 1\right) \cdot \frac{C_e}{C_m}\right]} \tag{12}$$

where $C_{BET}$ is the BET adsorption isotherm coefficient [L mg$^{-1}$], $C_m$ is the adsorbate mono-layer saturation concentration [mg L$^{-1}$], $S_m$ is the theoretical isotherm saturation capacity [mg g$^{-1}$] and $C_e$ is the equilibrium adsorption capacity [mg g$^{-1}$]. The BET model is considered a special

form of the Langmuir model, in which the layers after the first have the same energy (Foo and Hameed 2010).

Fits were performed with all models, but only physically meaningful results are reported in Table 3. For instance, for SA10-A1, it is apparent that a linear model with one parameter is sufficient to interpret the results with enough accuracy. Therefore, the fits obtained with models with two parameters (i.e., Langmuir and Freundlich models) are not reported because they are not considered physically meaningful. For the isotherms obtained for SA11-A4 and OA2-A1 samples, it is apparent that models with two or more parameters are necessary to better interpret the experimental results. Figure 4 shows the models that satisfactorily fit the experimental data.

For both aqueous solutions, all the models confirm the evidence from raw data that the order of affinity for caesium among the sandy sediment samples under study can be summarised and sketched as follows: SA11-A4 > SA10-A1 > OA2-A1.

## Discussion of kinetic tests and comparison with literature results

The analysis of the fits (Figs. 1 and 2) and the corresponding coefficient of determination values (see Supplementary Material) show that the experimental results are slightly better modelled by the pseudo-second-order model ($R^2 > 0.98$), which suggests two-sites-occupancy adsorption kinetics. This behaviour is consistent with the presence of illite in all the studied samples, which is characterised by having various different sites for caesium adsorption (Comans et al. 1991; Cornell 1993).

Kinetic results show that, irrespective of the association between the sand sample and mineral water, the adsorption kinetics appear to be characterised by a fast initial phase, during which a large fraction of the total amount of caesium ions originally present in the solution is removed, followed by a very slow removal phase (Figs. 1 and 2). This finding is in accordance with literature studies regarding the caesium adsorption process (Cornell 1993), which suggest that the initial removal from solution can be associated with ion exchange on the mineral surface. This process depends both on the concentration gradient existing between the bulk solution and boundary layer of the sorbent surface and on the initial availability of accessible external sites of the clay/micaceous minerals not yet occupied (Torstenfelt et al. 1982). For longer times, the removal rate reduces because caesium ions diffuse more slowly across the boundary layer and in micro fissures and because the fraction of the grain surface still available for adsorption reduces. It is also important to consider that sandy samples, such as the ones studied in this work, are characterised by a heterogeneous network of

**Table 3** Parameters of regression analyses of equilibrium isotherms data for the six associations between sandy samples and aqueous solutions

| Sample | Linear model | | Langmuir model | | | Freundlich model | | | BET model | | | |
|---|---|---|---|---|---|---|---|---|---|---|---|---|
| | $K_d$ [mL g$^{-1}$] | $R^2$ | $S_{max}$ [mg g$^{-1}$] | $K_L$ [L mg$^{-1}$] | $R^2$ | $1/n$ | $K_F$ [mg g$^{-1}$ (mg L$^{-1}$)$^{-1/n}$] | $R^2$ | $S_m$ [mg g$^{-1}$] | $C_{BET}$ [L mg$^{-1}$] | $C_m$ [mg L$^{-1}$] | $R^2$ |
| *Water A* | | | | | | | | | | | | |
| SA10-A1 | 311 | 0.989 | – | – | – | – | – | – | – | – | – | – |
| SA11-A4 | 1232 | 0.941 | – | – | – | 1.63 | 3.86 | 0.997 | 45 | 0.0089 | 0.613 | 0.994 |
| OA2-A1 | 78.5 | 0.840 | 0.36 | 0.64 | 0.995 | 0.575 | 0.125 | 0.970 | – | – | – | – |
| *Water V* | | | | | | | | | | | | |
| SA10-A1 | 124 | 0.982 | – | – | – | – | – | – | – | – | – | – |
| SA11-A4 | 750 | 0.827 | – | – | – | 2.33 | 5.16 | 0.991 | 34 | 0.0044 | 0.586 | 0.978 |
| OA2-A1 | 57 | 0.917 | 0.427 | 0.28 | 0.995 | 0.669 | 0.088 | 0.981 | – | – | – | – |

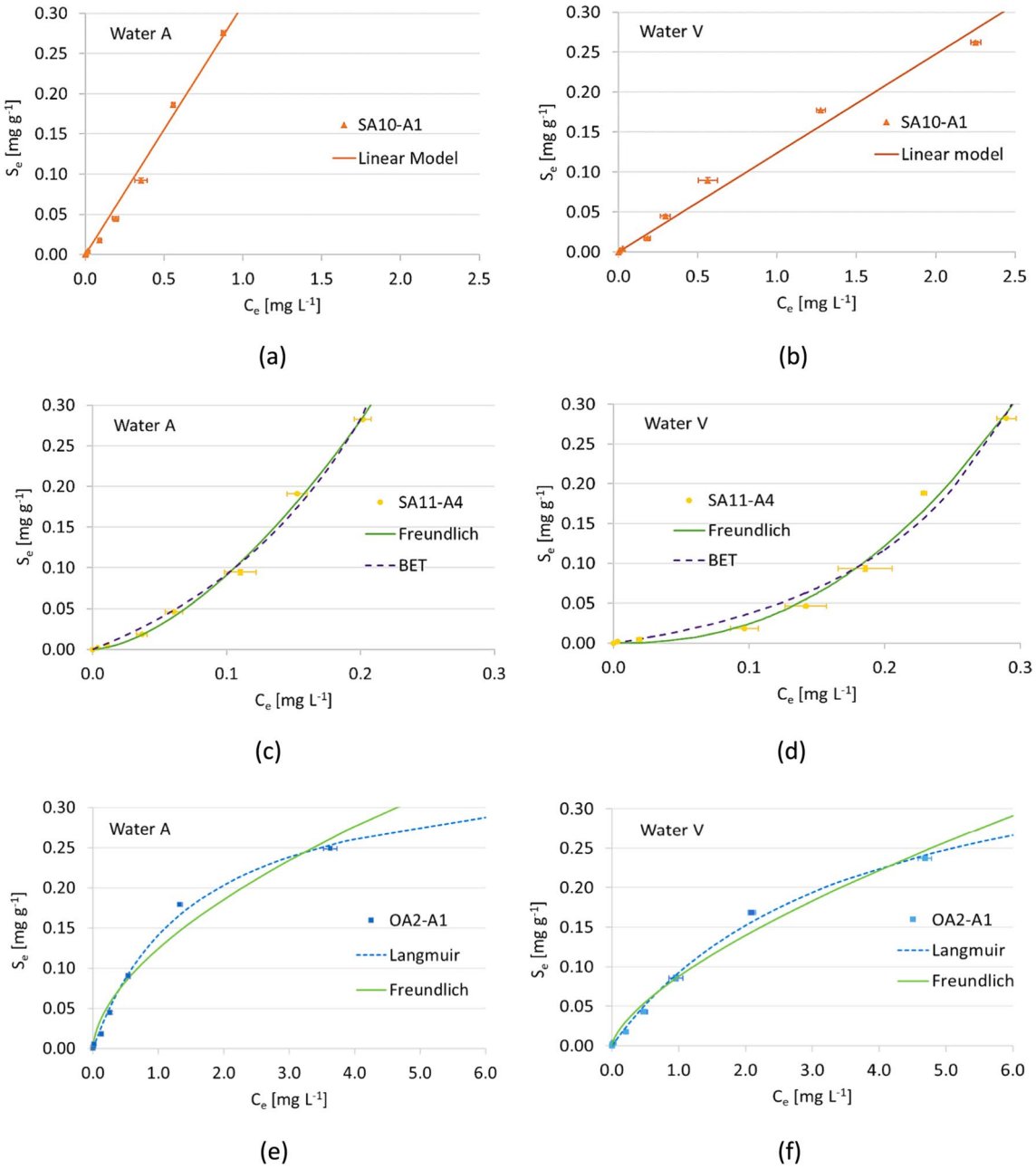


**Fig. 4** Equilibrium batch tests. Dots correspond to experimental data. Continuous lines and dashed lines correspond to the fits. **a** SA10-A1/water A; **b** SA10-A1/water V; **c** SA11-A/water A; **d** SA11-A/water V; **e** OA2-A1/water A; and **f** OA2-A1/water V

microfissures. Therefore, it can be supposed that initially, caesium ions easily diffuse inside larger ones and then slowly diffuse into smaller ones, which are more difficult to access. Indeed, taking into account the structure of the minerals responsible for the adsorption of caesium, the two-step kinetics could be explained by the initial process of occupation of abundant basal plane sites, followed by the increasing occupancy of high-affinity frayed edge sites of the interlayers (FES; Cornell 1993; Giannakopoulou et al. 2007).

Particularly, according to literature, the presence of micaceous and/or clayey minerals and/or calcite minerals, among which biotite or illite, involves an initial fast removal of caesium from solution, followed by a slower stage which can continue for days or even weeks (Comans et al. 1991; Cornell 1993; Gülten and Tuba 1996; Huitti et al. 2000).

The above-described behaviours are consistent with the results of this work's kinetic experiments. Micaceous minerals (illite) were observed in all the studied sediment samples (Table 1). Particularly, the relative amount of

micaceous minerals was observed to be the highest in the SA11-A4 sample (16 wt%), which shows faster kinetics and lower equilibrium times. Moreover, SA11-A4 also contains vermiculite (7.1 wt%), while calcite is present in the SA10-A1 and OA2-A1 sediment samples.

Shorter equilibrium times were observed with water A. This finding can be attributed to the very low content of dissolved electrolytes in water A and, therefore, to initial concentration differences between the solution and the matrix, which are higher than those of the tests with water V.

From the application of the empirical diffusion model of Weber and Morris (1963) to kinetic data (Fig. 3), two linear steps can be recognised in each of the performed experiments. It is generally accepted that the whole adsorption process consists of the following steps and processes (Li et al. 2010; Caccin et al. 2016):

1. Bulk diffusion (in solution)—ions diffuse from the bulk liquid to the liquid film or boundary layer surrounding the sorbent
2. Film diffusion—ions move from the boundary film to the external surface of the sorbent
3. Particle diffusion (in the solid phase)—ions transfer from the surface to the intra-particle active sites
4. Adsorption reaction—ions are adsorbed by the active sites of the sorbent.

Since the adsorption reaction is a very rapid step and the bulk diffusion is a process which depends on the diffusion coefficient of the ions under consideration and not from the sorbent, in general, the rate-limiting steps are the second and third steps (i.e., film and particle diffusion processes; Li et al. 2010). Therefore, according to this simplified model, caesium adsorption kinetics onto the sandy samples might be interpreted as a rate limited by two processes: an initial film diffusion followed by a slower intra-particle diffusion.

From the estimated equilibrium times reported in Table 4 and from the fits (Figs. 1 and 2 and Supplementary Material), the adsorption of caesium is faster onto the SA11-A4 sample, which is also the one characterised by a higher amount and variety of clay and micaceous minerals in the mud component.

Moreover, the time variations in the concentrations of Na, Mg, K, Ca and Sr, for the six associations of sandy samples and mineral water (Supplementary Material), in the absence and in the presence of caesium in solution, demonstrate that all the observed adsorption and desorption processes over time are not affected by the absence or presence of caesium in solution. This finding indicates the absence of any detectable competitive behaviour between Cs and other ions present in the aqueous stock solutions in the range of concentrations considered here.

Table 4 lists the results of existing studies' kinetic experiments of caesium ions adsorption onto sandy samples performed in conditions similar to those of this work. Particularly, Table 4 includes information about the composition of the porous media and aqueous solutions, pH and equilibrium times to be compared with the results of the present study.

The equilibrium times observed in this study are much greater than the values obtained in most of the previous studies listed in Table 4. The comparison of data in this paper and existing literature suggests this finding could be partially attributed to the relatively small quantity of clay fraction contained in the sandy samples studied and the grain size distribution of the sediments.

In general, long equilibrium times could be of concern regarding the capability of such matrices to actually delay caesium migration in the case of relatively high advective groundwater flow rates. The delay effect, due to the high affinity between the matrix and the solute, is usually modelled by supposing instantaneous equilibrium in the sorption process. This assumption can be considered valid if groundwater flow is so slow that the solute can be considered almost immobile with respect to the adsorption characteristic time. However, if the characteristic time of groundwater flow is comparable to or even higher than the characteristic time of adsorption processes, equilibrium conditions can no longer be considered valid and non-equilibrium exchanging processes need to be included in modelling tools to avoid overestimates of the delay of the contaminant-front arrival time (Giacobbo and Patelli 2007).

## Discussion of equilibrium batch tests and comparison with literature

The results of the fits, reported in Table 3 and Fig. 4, show the following properties with both waters A and V in the range of initial caesium concentrations considered: (i) SA10-A1 sample isotherms are satisfactorily fitted by linear models; (ii) SA11-A4 sample isotherms show a particular trend that can be fitted either with a Freundlich model with $1/n > 1$, which suggests the occurrence of cooperative adsorption processes, or with a BET model which refers to multi-layer adsorption processes; and (iii) OA2-A1 sample isotherms are well fitted by both Freundlich and Langmuir models, with a slight difference between the two, making a mono-layer adsorption process slightly more probable than a multi-layer one.

Particularly, the complex behaviour of SA11-A4 isotherms is confirmed by a specific analysis of the data. The plot of measurements and fitting models with a log–log scale (Fig. 5) clearly shows that the data for the smallest values of $C_e$, namely for $C_e < 0.1$ mg $L^{-1}$, are better fitted by the BET model, rather than by the Freundlich one, even if $R^2$ values for the whole data set differ only slightly (Table 3). The latter

**Table 4** Literature studies, showing equilibrium times of caesium adsorption onto sandy samples

| Solid matrix grain size distribution | Soil and mineral phase* (%) | Background aqueous and soluble cations concentration of cations in mg $L^{-1}$ | Solution pH | Equilibrium time | Reference |
|---|---|---|---|---|---|
| 96% sand<br>4% silt<br>< 1% clay | Qz = 50 to 55;<br>Kfs = 15 to 20<br>Hbl + Px = 20 to 25<br>Grt = 5 to 10;<br>Bt + Ms = 1 | Site-specific groundwater<br>$Ca^{2+}$ = 5.1; $Na^{+}$ = 11;<br>$Mg^{2+}$ = 1.9; $K^{+}$ = 3.2 | 6.9 | 16 h | (Reynolds et al. 1982) |
| 34 ÷ 62% sand<br>20 ÷ 24% silt<br>12 ÷ 14% clay | Qz, Ilt, Vrm | Electrolyte solution<br>($CaCl_2$ = 0.01 mol $L^{-1}$)<br>$Ca^{2+}$ = 400.8 | 5–10 | 16 h | (Giannakopoulou et al. 2007) |
| Coarse sand to Fine sand | Qz | Water (further information n.a.) | > 8.1 | 8 h | (Hassan 2016) |
| Clay coarse sand | Qz, Cal, Dol, Mnt | Site-specific groundwater<br>$Ca^{2+}$ = 605; $Na^{+}$ = 2075;<br>$Mg^{2+}$ = 137; $K^{+}$ = 0.02 | 7.6 to 8.6 | 2 h | (El-Reefy et al. 1994) |
| Sandy loam<br>62% sand<br>24% silt<br>14% clay | Qz, Ilt, Kln | Electrolyte solution<br>($CaCl_2$ = 0.01 mol $L^{-1}$)<br>$Ca^{2+}$ = 400.8 | 7 | 16 h | (Giannakopoulou et al. 2012) |
| Sandy soil<br>96.1% sand<br>3.6% silt/clay | Qz, Pl, Kfs, Chl | Deionised water | 7 | 56 d | (Tanaka and Ohnuki 1994) |
| SA10-A1<br>96.42% sand<br>0.11% gravel<br>3.47% mud (silt + clay) | Dol, Qz, M (Ilt), Chl, Cal, Kfs | Water A<br>$Ca^{2+}$ = 4.4; $Na^{+}$ = 2.6;<br>$Mg^{2+}$ = 0.6; $K^{+}$ = 4.4 | 7.4 | 7 d | This study |
| | | Water V<br>$Ca^{2+}$ = 88.7; $Na^{+}$ = 4.3;<br>$Mg^{2+}$ = 34.8; $K^{+}$ = 5.6 | 8.0 | 10 d | |
| SA11-A4<br>98.4% sand<br>1.6% mud (silt + clay) | Qz, M (Ilt), Chl, Kfs, Dol, Amp, Vrm | Water A<br>$Ca^{2+}$ = 4.4; $Na^{+}$ = 2.6;<br>$Mg^{2+}$ = 0.6; $K^{+}$ = 4.4 | 7.4 | 1 d | This study |
| | | Water V<br>$Ca^{2+}$ = 88.7; $Na^{+}$ = 4.3;<br>$Mg^{2+}$ = 34.8; $K^{+}$ = 5.6 | 8.0 | 7 d | |
| OA2-A1<br>92.1% sand<br>2.72% gravel<br>5.18% mud (silt + clay) | Qz, Dol, M (Ilt), Cal, Chl, Kfs | Water A<br>$Ca^{2+}$ = 4.4; $Na^{+}$ = 2.6;<br>$Mg^{2+}$ = 0.6; $K^{+}$ = 4.4 | 7.4 | 5 d | This study |
| | | Water V<br>$Ca^{2+}$ = 88.7; $Na^{+}$ = 4.3;<br>$Mg^{2+}$ = 34.8; $K^{+}$ = 5.6 | 8.0 | 10 d | |

*Abbreviations for names of rock-forming minerals (Whitney and Evans 2010): *Amp* amphibole, *Bt* biotite, *Cal* calcite, *Chl* chlorite, *Dol* dolomite, *Grt* garnet, *Hbl* hornblende, *Ilt* illite, *Kfs* K-feldspar, *Kln* kaolinite, *Mnt* Montmorillonite, *Ms* muscovite, *Pl* plagioclase, *Px* pyroxene, *Qz* quartz, *Vrm* vermiculite, *M* undifferentiated micas

remark can be justified by the fact that the relative error on the smallest values of $C_e$ could be relatively great, as visible from Fig. 5, but absolute residuals are nevertheless small and have a limited impact on the computation of $R^2$.

It is also important to stress that the values of the parameters of the BET model are not identified with a low uncertainty. The objective function to be minimised with the non-linear least-squares approach, which has been applied here, is rather flat for a wide range of values so that different sets of fitting parameters would give the same agreement between the model outcomes and the data. This could only be partially mitigated by collecting additional data in the examined range of Ce because the trend is nevertheless clear. The collection of data over a range of $C_e$ spanning more than three orders of magnitude could instead be useful to improve the assessment of different models.

The main message from the modelling of isotherms is the evidence of the complexity of adsorption processes for SA11-A4 sample. The most relevant results are the following: simple models (linear and Langmuir) cannot reproduce the trend of the isotherms for the SA11-A4 sample; the Freundlich model performs better but is still not fully

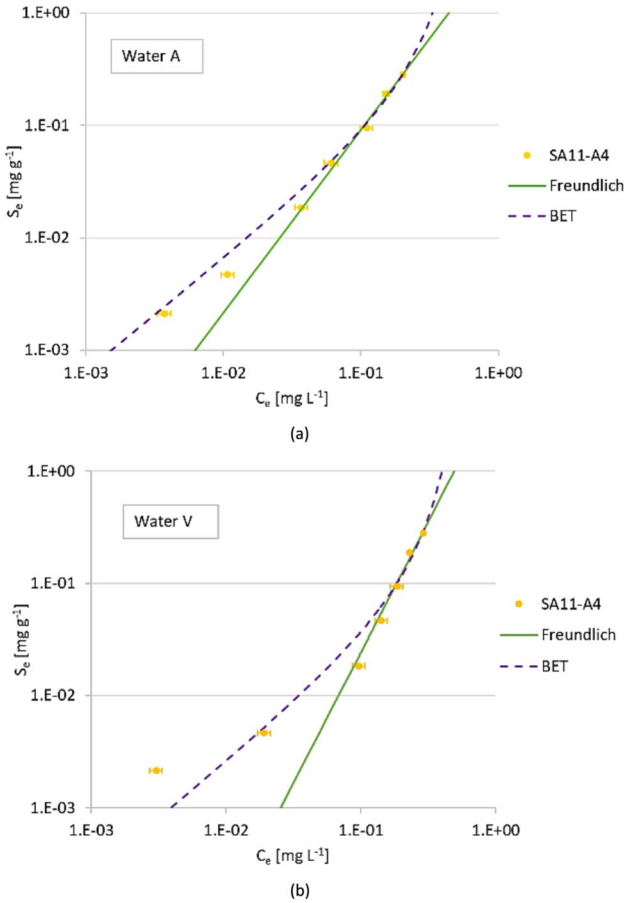


**Fig. 5** Caesium adsorption equilibrium isotherms onto **a** SA11-A4 with water A and **b** SA11-A4 with water V. Dots correspond to experimental data. Continuous lines and dashed lines correspond to Freundlich and BET isotherm models, respectively

satisfactory; and a complex model, like the BET model, would be necessary to fit the data over several orders of magnitude of $C_e$. Results are expected to be only modestly influenced by other processes like dissolution and precipitation in the tested range of concentrations and for the physico-chemical conditions under which the experiments have been performed.

Regardless of the type of aqueous solution and the isotherm model, the order of affinity for caesium among the sandy samples under study can be summarised and sketched as follows: SA11-A4 > SA10-A1 > OA2-A1.

This result is consistent with the observed higher amount and variety of clay and micaceous minerals in the SA11-A4 sample (Table 1). This finding is also coherent with the measurements of CEC and the specific surface area of the three samples (Table 1). The CEC of SA11-A4 is greater than that of the other samples by about 50%; moreover, the specific surface area for SA11-04 and for OA2-A1 is the greatest and the smallest, respectively, for the three samples.

Moreover, the particular trend of caesium equilibrium isotherms onto SA11-A4 (fitted with the Freundlich model with $1/n > 1$ or with a BET model) may also be ascribed to the higher variety of clay and micaceous minerals and to the higher amount of illite present in the sample. According to the literature, the adsorption of caesium onto illite can be interpreted with multi-site ion exchange models due to the presence of various adsorption sites (Comans et al. 1991; Cornell 1993).

The comparison of adsorption isotherms obtained with the two different aqueous solutions characterised by different contents of dissolved solids may enable the investigation of the influence of total dissolved solids on caesium uptake. In general, it is expected that the caesium uptake would be lower in an aqueous solution with higher ionic strength (i.e., water V) with respect to an aqueous solution with a lower ionic strength (i.e., water A). This finding is confirmed by the results shown in Fig. 4.

In Fig. 6, equilibrium batch results obtained in the present study are compared with selected studies of literature involving similar solid matrices, either single minerals or a mixture of minerals, different ranges of caesium initial concentrations and different aqueous solutions. Some studies on competition are included in the reported literature results. The details of the batch experiments, which refer to the equilibrium isotherms shown in Fig. 6, are listed in Table 5.

In Fig. 6, data are plotted in a bi-logarithmic scale so that equilibrium adsorption data, which can be fitted by linear and Freundlich models, would appear positioned along straight lines with different slopes. Namely, linear isotherms would appear as lines with angular coefficient equal to 1, whereas Freundlich isotherms would appear as lines with different slopes depending on the *1/n* exponent of Eq. (10), as shown by Eq. (11).

Data referring to experiments performed with samples characterised by a mixture of different minerals are reported with circles in Fig. 6, whereas triangles refer to experiments performed with single minerals.

As shown in the subplot of Fig. 6, in the selected range, the data obtained in the present work follow a trend similar to the results of the literature, which refer to sandy samples with some portions of clay and mica. See, for instance, the results by Reynolds et al. (1982) for a natural sandy sample from Canada (acronym R) and by Tanaka and Ohnuki (1994) for a silica sand sample (acronym TA). A good agreement is observed with the results for micaceous sediments, which are richer in clay than the samples under consideration but whose behaviour was examined in the presence of competing ions so that caesium sorption was limited (acronym Z; Zachara et al. 2002). In the subplot of Fig. 6, data referring to pure illite samples saturated by K and Na show a trend similar to the data of the present work but with higher adsorption (acronym ST; Staunton and Roubaud 1997).

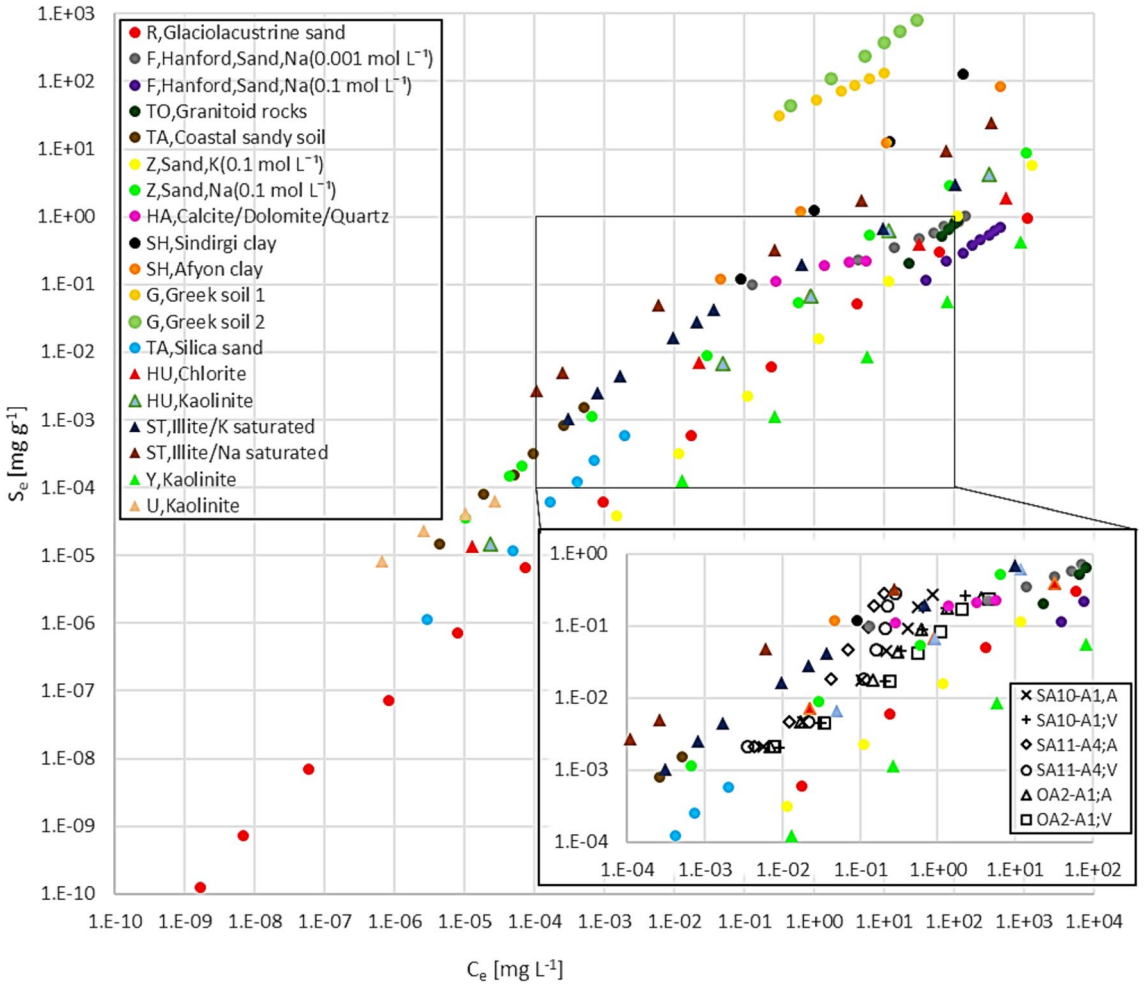


**Fig. 6** Caesium adsorption onto different matrices. A comparison of literature batch studies at equilibrium. Capital letters in the legend refer to the acronyms listed in Table 5. Triangles represent studies with single mineral matrices, whereas circles represent studies with matrices characterised by a mixture of minerals. The results of the present study are shown with black symbols in the exploded view. The results refer to the three sandy samples SA10-A1, SA11-A4 and OA2-A1 in contact with the two aqueous solutions of the present study, which are indicated with 'A' and 'V' letters

Figure 7 focuses on the range of caesium concentrations considered in the present study and on the results obtained with water V, which is the water that better represents the groundwater composition of the region from which the sandy samples were taken.

Data reported in Fig. 7 have been interpolated with the linear isotherm model to facilitate an overall comparison in terms of distribution coefficient values, $K_d$. Particularly, the selected literature experiments have been performed under conditions (i.e., simulated or real groundwater as solvent) and a range of caesium $C_e$ (i.e., between $10^{-4}$ and $10^{2}$ mg $L^{-1}$) similar to those of this study. Then, the results of those experiments can be compared with those obtained in the present study with water V, which is richer in salts than water A and, therefore, more similar to real groundwater conditions. The comparison of obtained $K_d$ values is reported in Table 6. It is important to point out that these $K_d$ values have been obtained by considering a portion of the literature data, namely, that in the range of caesium concentration in solution at equilibrium from $10^{-4}$ to 100 mg $L^{-1}$, which corresponds to the range examined within the experiments of this work.

From this analysis, it can be observed that $K_d$ values corresponding to the associations between sediment samples and water V vary between 57 and 750 mg $L^{-1}$; therefore, the range covers more than one order of magnitude. The obtained values are also in accordance with the range of between 100 and 1000 mg $L^{-1}$ for $K_d$ values suggested for pure sand soils by Sheppard (1990).

**Table 5** Experimental data and references of literature caesium adsorption tests reported in Fig. 6

| Acronym | Site | Solid matrix | Mineralogy* | Liquid phase concentration of cations in mg $L^{-1}$ | Comments | References |
|---|---|---|---|---|---|---|
| *Mixed minerals* | | | | | | |
| R | Canada | 96% sand<br>4% silt<br>< 1% clay | Sand fraction:<br>Qz; Kfs; Hbl, Px; Grt; Bt; Ms | Site-specific groundwater<br>$Ca^{2+}$ = 5.1;<br>$Na^{+}$ = 11;<br>$Mg^{2+}$ = 1.9;<br>$K^{+}$ = 3.2 | Linear isotherm | (Reynolds et al. 1982) |
| F | USA | 95% sand<br>4% silt<br>1% clay | Sand fraction:<br>Qz; Amp; Pl; Kfs; M; Mag<br>Clay fraction:<br>Chl; Sme; Vrm; Kln; Ilt; Qz | Electrolyte solution (NaCl = 0.001 mol $L^{-1}$)<br>$Na^{+}$ = 22.99<br>Electrolyte solution (NaCl = 0.1 mol $L^{-1}$)<br>$Na^{+}$ = 2299 | Freundlich isotherm | (Flury et al. 2004) |
| TO | Sweden | Crushed granitoid rock | Qz; Pl; Fsp; M; Ms; Chl | Synthetic groundwater<br>$Ca^{2+}$ = 18.0;<br>$Mg^{2+}$ = 4.3;<br>$Na^{+}$ = 6.5;<br>$K^{+}$ = 3.9 | | (Toshiaki 1984) |
| TA | Japan | Coastal sandy soil | Qz; Pl; Kfs; Hbl; Ser; Chl | Deionised water | Linear isotherm | (Tanaka and Ohnuki 1994) |
| Z | USA | 89.3% sand,<br>9.3% clay,<br>1.4% gravel | Sand fraction:<br>Qz; Chl; Pl; Kfs; M; Bt; Ms<br>Clay fraction:<br>Chl; Sme; M | Electrolyte solution ($KNO_3$ = 0.1 mol $L^{-1}$)<br>$K^{+}$ = 3910<br>Electrolyte solution ($NaNO_3$ = 0.1 mol $L^{-1}$) $Na^{+}$ = 2299 | Competition study | (Zachara et al. 2002) |
| HA | Egypt | Marble | Cal; Qz; Dol; Gp; Fsp | Double distilled water | Langmuir isotherm | (Hamed et al. 2016) |
| G | Greece<br>Soil 1 | 62% sand<br>24% silt<br>14% clay | Qz, other undifferentiated minerals | Electrolyte solution ($CaCl_2$ = 0.01 mol $L^{-1}$)<br>$Ca^{2+}$ = 400.8 | Freundlich isotherm<br>Soil with a high percentage of mud | (Giannakopoulou et al. 2007) |
| | Greece<br>Soil 2 | 48% sand<br>40% silt<br>12% clay | Qz, other undifferentiated minerals | | | |
| SH | Turkey | Natural clay mineral | Kln; Qz | Tap water<br>$Ca^{2+}$ = 6.49;<br>$Mg^{2+}$ = 5.23<br>$Na^{+}$ = 9.01;<br>$K^{+}$ = 4.07 | Freundlich isotherm<br>Reference temperature 30 °C | (Shahwan and Erten 2002) |
| | | Natural clay mineral | Chl + Ilt mixed clay; Cal; Qz | | | |
| SA10-A1 | Northern Italy | 96.42% sand<br>0.11% gravel<br>3.47% (silt + clay) | Dol, Qz, M (Ilt), Chl, Cal, Kfs | Water A<br>$Ca^{2+}$ = 4.4;<br>$Na^{+}$ = 2.6;<br>$Mg^{2+}$ = 0.6;<br>$K^{+}$ = 4.4 | Linear isotherm | This study |
| | | | | Water V<br>$Ca^{2+}$ = 88.7;<br>$Na^{+}$ = 4.3;<br>$Mg^{2+}$ = 34.8;<br>$K^{+}$ = 5.6 | Linear isotherm | |

**Table 5** (continued)

| Acronym | Site | Solid matrix | Mineralogy* | Liquid phase concentration of cations in mg $L^{-1}$ | Comments | References |
|---|---|---|---|---|---|---|
| SA11-A4 | Northern Italy | 98.4% sand<br>1.6% (silt + clay) | Qz, M (Ilt), Chl, Kfs, Dol, Amp, Vrm | Water A<br>$Ca^{2+}$ = 4.4;<br>$Na^{+}$ = 2.6;<br>$Mg^{2+}$ = 0.6;<br>$K^{+}$ = 4.4 | Freundlich and BET isotherms | This study |
| | | | | Water V<br>$Ca^{2+}$ = 88.7;<br>$Na^{+}$ = 4.3;<br>$Mg^{2+}$ = 34.8;<br>$K^{+}$ = 5.6 | Freundlich and BET isotherms | |
| OA2-A1 | Northern Italy | 92.1% sand<br>2.72% gravel<br>5.18% (silt + clay) | Qz, Dol, M (Ilt), Cal, Chl, Kfs | Water A<br>$Ca^{2+}$ = 4.4;<br>$Na^{+}$ = 2.6;<br>$Mg^{2+}$ = 0.6;<br>$K^{+}$ = 4.4 | Freundlich and Langmuir isotherm | This study |
| | | | | Water V<br>$Ca^{2+}$ = 88.7;<br>$Na^{+}$ = 4.3;<br>$Mg^{2+}$ = 34.8;<br>$K^{+}$ = 5.6 | Freundlich and Langmuir isotherm | |
| *Single minerals* | | | | | | |
| HU | Finland | Granite (fracture minerals) | Chl<br>Kln | Simulated fresh groundwater<br>$Ca^{2+}$ = 12;<br>$Mg^{2+}$ = 2.8;<br>$Na^{+}$ = 53;<br>$K^{+}$ = 3.9; Cl = 50;<br>$SO_4$ = 9.6;<br>$SiO_2$ = 2.9;<br>$HCO_3$ = 91 | Non-linear adsorption | (Huitti et al. 2000) |
| TA | Japan | Sand | Silica | Deionised water | Linear isotherm | (Tanaka and Ohnuki 1994) |
| ST | France | Clay | Ilt | Electrolyte solution (KCl = 0.1 mol $L^{-1}$)<br>$K^{+}$ = 3910<br>Electrolyte solution (NaCl = 0.1 mol $L^{-1}$)<br>$Na^{+}$ = 2299 | Freundlich isotherm<br>Liquid phase rich in salts (competition study) | (Staunton and Roubaud 1997) |
| Y | Turkey | Clay | Kln | Synthetic groundwater<br>$Ca^{2+}$ = 5210.14;<br>$Mg^{2+}$ = 60,033;<br>$Na^{+}$ = 11,495;<br>$K^{+}$ = 1954.9 | Freundlich isotherm<br>Reference temperature 5 °C<br>Liquid phase rich in salts<br>(competition study) | (Yildiz et al. 2011) |
| U | Turkey | Clay | Kln | Deionised water | Freundlich and Langmuir Isotherm | (Ugur and Sahan 2012) |

*Abbreviations for names of rock-forming minerals (Whitney and Evans 2010): *Amp* amphibole, *Bt* biotite, *Cal* calcite, *Chl* xhlorite, *Dol* dolomite, *Fspx* felspar, *Grt* garnet, *Gp* gypsum, *Hbl* hornblende, *Ilt* illite, *Kfs* K-feldspar, *Kln* kaolinite, *Mag* magnetite, *Mnt* montmorillonite, *Ms* muscovite, *Pl* plagioclase, *Px* pyroxene, *Qz* quartz, *Ser* sericite, *Srp* serpentine, *Vrm* vermiculite, *M* undifferentiated mica

## Conclusion

Kinetic and equilibrium batch tests were carried out for six different associations of three alluvial sediment samples from the Po Plain (Italy) and aqueous solutions with two commercial mineral waters as solvent and caesium as solute. The initial solutions contained caesium in the range between 0.25 and 30 mg $L^{-1}$. Kinetic and equilibrium data were then fitted by kinetic and isotherm models. The studied sandy samples showed a high affinity for caesium ions.

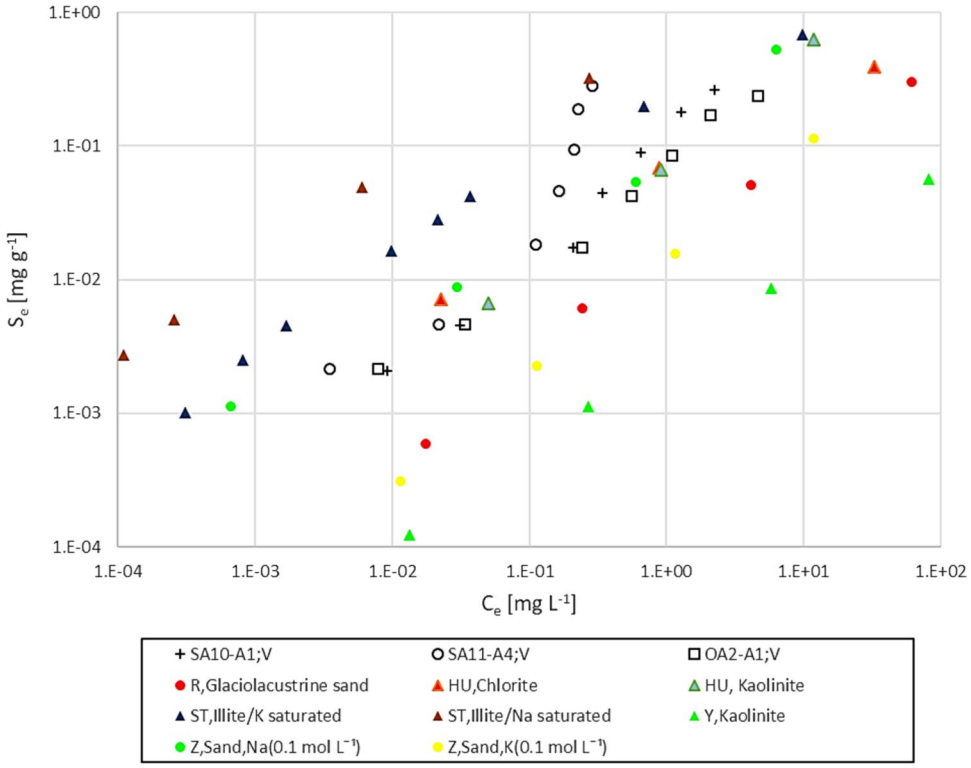


**Fig. 7** Comparison of caesium adsorption batch experiments of the present work with different solid matrices of literature (Table 6). Black crosses, open circles and squares refer to the experimental data of this work obtained with the three sandy samples SA10-A1, SA11-A4 and OA2-A1 in contact with water V

**Table 6** $K_d$ values of caesium adsorption equilibrium tests of the data sets shown in Fig. 7

| Predominant mineral | Figure 7 label | Aqueous solution | $K_d$ [mL g$^{-1}$] | References |
|---|---|---|---|---|
| Clay | ST, illite Na-saturated | Solution rich in salts | 1382 | (Staunton and Roubaud 1997) |
| Sand | SA11-A4; V | Water V | 750 | This work |
| Clay | ST, illite K-saturated | Solution rich in salts | 386 | (Staunton and Roubaud 1997) |
| Sand | SA10-A1; V | Water V | 124 | This work |
| Clay | HU, chlorite | Simulated fresh groundwater | 98 | (Huitti et al. 2000) |
| Sand | Z, Na (0.1 mol L$^{-1}$) | Solution rich in salts | 88 | (Zachara et al. 2002) |
| Sand | OA2-A1; V | Water V | 57 | This work |
| Clay | HU, kaolinite | Simulated fresh groundwater | 51 | (Huitti et al. 2000) |
| Sand | R, glaciolacustrine sand | Groundwater | 13 | (Reynolds et al. 1982) |
| Sand | Z, K (0.1 mol L$^{-1}$) | Solution rich in salts (competition study) | 9.5 | (Zachara et al. 2002) |
| Clay | Y, kaolinite | Solution rich in salts (competition study) | 0.7 | (Yildiz et al. 2011) |

Results with water V only are considered here. Labels in the second column refer to the acronyms listed in Fig. 7

The two aqueous solutions were selected in order to comply with the characteristics of groundwater in the area where sediment samples were collected (water V) or to have a low content of dissolved ions (water A). As could be expected, the caesium adsorption was less remarkable for the solutions obtained with water V, which was characterised by a higher content of dissolved solids with respect to water A This finding suggests that in the presence of high concentrations of dissolved solids (i.e., ions competing with caesium for adsorption sites), this phenomenon could be more accentuated and the caesium uptake could be reduced in a significant way, as observed in literature with other matrices.

Differences among the three samples in the kinetic and equilibrium batch test results were instead quite relevant, consistent with measurements of CEC and specific surface area, and possibly related to differences in the clay content and composition. The results show that even a small fraction of clay minerals permits relevant adsorption of caesium and that the mixtures of such minerals may introduce a complex behaviour, which can be described by very different models.

Observed equilibrium times are relatively long with respect to analogous literature results. This is very relevant for safety assessment because it might imply that transport processes could occur under non-equilibrium conditions. Therefore, a more in-depth analysis is necessary to find proper models which can effectively describe non-equilibrium adsorption processes.

The present work is the first part of a research project aimed at studying the adsorption of caesium onto natural sediment samples from the Italian territory both under static and dynamic conditions using batch and column experiments and in presence of competitive ions that are typically released with caesium due to dissolution of the barrier system. The experimental results will enable the determination of rates that can be adopted for simulation purposes. The results of the present work set a good reference for analysing the effects of the presence of competing ions (e.g., potassium and/or sodium) on caesium adsorption. Therefore, future developments will be devoted to the study of caesium adsorption and desorption onto and from the same sediment samples, with the same waters, in the presence of competing ions. Future studies will also focus on identifying the appropriate models that can be adopted to describe non-equilibrium adsorption and related adsorption/desorption rates.

**Supplementary Information** The online version contains supplementary material available at https://doi.org/10.1007/s13762-024-05814-2.

**Acknowledgements** The authors are grateful to the Laboratory for Radioactive Measurements of the Joint Research Centre (JRC) of Ispra for availability of equipment, to the Dipartimento di Scienze agrarie e ambientali – DISAA of the Università degli Studi di Milano, in the persons of Prof. Gian Attilio Sacchi and Dott. Giorgio Lucchini, for support and to the Radiochemistry and Radiation Chemistry Lab of the Nuclear Engineering division of the Politecnico di Milano for availability of equipment for preliminary evaluations. Prof. Fulvia Tambone is thankfully acknowledged for support in the CEC measurements. Dr. Silvia Inzoli is thankfully acknowledged for providing the sandy samples and for discussion on their petrophysical and sedimentological properties. Dr. Francesco Galluccio is thankfully acknowledged for his kind help.

**Author contributions** Francesca Giacobbo and Mauro Giudici were responsible of the study conception and design and supervised all steps of the research. Federica Pezzoli curated the bibliographic review, in particular the collection of published data. Material preparation, data acquisition and analysis for batch tests were performed by Federica Pezzoli and Mirko Da Ros. Izabela Cydzik contributed to ICPMS measurements at JRC. Monica Dapiaggi contributed to the analysis of XRD data and geochemical analysis. The first draft of the manuscript was written by Francesca Giacobbo, while Mirko Da Ros draw the figures. All authors commented on previous versions of the manuscript, and read and approved the final manuscript.

**Funding** Open access funding provided by Politecnico di Milano within the CRUI-CARE Agreement. This research did not receive any specific grant from funding agencies in the public, commercial, or not-for-profit sectors. Prof. Mauro Giudici and Prof. Monica Dapiaggi performed this research partially in the framework of the project "Geosciences for society: resources and their evolution" supported by the Italian Ministry of University and Research (MUR) through the fund 'Dipartimenti di Eccellenza 2018–2022'.

## Declarations

**Conflict of interest** The authors have no relevant financial or non-financial interests to disclose.

**Ethical approval** Not applicable.

**Consent to participate** Not applicable.

**Consent for publication** Not applicable.



## References

ASTM C1733–17a. Standard test method for distribution coefficients of inorganic species by the batch method. Last Updated 2021. https://standards.globalspec.com/std/4058632/astm-c1733-17a.

Ayawei N, Ebelegi AN, Wankasi D (2017) Modelling and interpretation of adsorption isotherms. J Chem 2017:1–11. https://doi.org/10.1155/2017/3039817

Benedicto A, Missana T, Fernández AM (2014) Interlayer collapse affects on cesium adsorption onto illite. Environ Sci Technol 48(9):4909–4915. https://doi.org/10.1021/es5003346

Bouzidi A, Souahi F, Hanini S (2010) Sorption behavior of cesium on Ain Oussera soil under different physicochemical conditions. J Hazar Mater 184(1–3):640–646. https://doi.org/10.1016/j.jhazmat.2010.08.084

Caccin M, Giacobbo F, Da Ros M, Besozzi L, Mariani M (2013) Adsorption of uranium, cesium and strontium onto coconut shell activated carbon. J Radioanal Nucl Chem 297:9–18. https://doi.org/10.1007/s10967-012-2305-x

Caccin M, Giorgi M, Giacobbo F, Da Ros M, Besozzi L, Mariani M (2016) Removal of lead (II) from aqueous solutions by adsorption onto activate carbons prepared from coconut shell. Desalin Water Treat 57(10):4557–4575. https://doi.org/10.1080/19443994.2014.992974

Carbol P, Engkvist I (1997) Compilation of radionuclide sorption coefficients for performance assessment. SKB Swedish Nuclear Fuel and Waste Management Co, SKB rapport R-97–13. https://www.skb.com/publication/13614/R-97-13.pdf

Cherif MA, Martin-Garin A, Gérard F, Bildstein O (2017) A robust and parsimonious model for caesium sorption on clay minerals and natural clay materials. Appl Geochem 87:22–37. https://doi.org/10.1016/j.apgeochem.2017.10.017

Ciesielski H, Sterckeman T, Santerne M, Willery JP (1997) A comparison between three methods for the determination of cation exchange capacity and exchangeable cations in soils. Agronomie 17(1):9–16. https://doi.org/10.1051/agro:19970102

CNAPI (Carta Nazionale delle Aree Potenzialmente Idonee) (2020). Deposito Nazionale, SOGIN S.p.A. Italy. https://www.depositonazionale.it/documenti/pagine/documenti-proposta-cnapi.aspx

Comans RNJ, Haller M, De Preter P (1991) Sorption of cesium on illite: Non-equilibrium behaviour and reversibility. Geochim Cosmochim Acta 55:433–440. https://doi.org/10.1016/0016-7037(91)90002-M

Cornell RM (1993) Adsorption of cesium on minerals: a review. J Radioanal Nucl Chem 171:483–500. https://doi.org/10.1007/BF02219872

Ding DH, Zhang ZY, Lei ZF, Yang YN, Cai TM (2016) Remediation of radiocesium-contaminated liquid waste, soil, and ash: a mini review since the Fukushima Daiichi nuclear power plant accident. Environ Sci Pollut Res 23:2249–2263. https://doi.org/10.1007/s11356-015-5825-4

Durrant CB, Begg JD, Kersting AB, Zavarin M (2018) Cesium sorption reversibility and kinetics on illite, montmorillonite, and kaolinite. Sci Total Environ 610–611:511–520. https://doi.org/10.1016/j.scitotenv.2017.08.122

Ebadi A, Soltan Mohammadzadeh JS, Khudiev A (2009) What is the correct form of BET isotherm for modeling liquid phase adsorption? Adsorption 15:65–73. https://doi.org/10.1007/s10450-009-9151-3

El-Reefy SA, Marei SA, Maghrawy HB, Aly A (1994) Interaction of Cesium, Cobalt and Americium with Sediments and Rocks of Inshas Site. In: Second Arab Conference on the Peaceful Uses of Atomic Energy, Cairo, 5–9 Nov. https://inis.iaea.org/collection/NCLCollectionStore/_Public/28/031/28031721.pdf

Endo S, Kimura S, Takatsuji T, Nanasawa K, Imanaka T, Shizuma K (2012) Measurement of soil contamination by radionuclides due to the Fukushima Dai-ichi Nuclear Power Plant accident and associated estimated cumulative external dose estimation. J Environ Radioact 111:18–27. https://doi.org/10.1016/j.jenvrad.2011.11.006

EPA (1999) Understanding variation in partition coefficient, Kd, values. Volume II. United States Environmental Protection Agency. https://www.epa.gov/sites/default/files/2015-05/documents/402-r-99-004b.pdf.

Ferreira DR, Thornhill JA, Roderick EIN, Li Y (2018) The impact of pH and Ion exchange on $^{133}$Cs adsorption on vermiculite. J Environ Qual 47:1365–1370. https://doi.org/10.2134/jeq2018.01.0043

Flury M, Czigany S, Chen G, Harsh JB (2004) Cesium migration in saturated silica sand and Hanford sediments as impacted by ionic strength. J Contam Hydrol 71:111–126. https://doi.org/10.1016/j.jconhyd.2003.09.005

Foo KY, Hameed BH (2010) Insights into the modeling of adsorption isotherm systems. Chem Eng J 156(1):2–10. https://doi.org/10.1016/j.cej.2009.09.013

Fuller AJ, Shaw S, Peacock CL, Trivedi D, Small JS, Abrahamsen LG, Burke IT (2014) Ionic strength and pH dependent multi-site sorption of Cs onto a micaceous aquifer sediment. Appl Geochem 40:32–42. https://doi.org/10.1016/j.apgeochem.2013.10.017

Fuller AJ, Shaw S, Ward MB, Haigh SJ, Mosselmans JFW, Peacock CL, Stackhouse S, Dent AJ, Trivedi D, Burke IT (2015) Caesium incorporation and retention in illite interlayers. Appl Clay Sci 108:128–134. https://doi.org/10.1016/j.clay.2015.02.008

Giacobbo F, Patelli E (2007) Monte Carlo simulation of nonlinear reactive contaminant transport in unsaturated porous media. Ann Nucl Energy 34(1–2):51–63. https://doi.org/10.1016/j.anucene.2006.11.011

Giannakopoulou F, Haidouti C, Chronopoulou A, Gasparatos D (2007) Sorption behavior of cesium on various soils under different pH levels. J Hazard Mater 149:553–556. https://doi.org/10.1016/j.jhazmat.2007.06.109

Giannakopoulou F, Gasparatos D, Haidouti C, Massas I (2012) Sorption Behavior of Cesium in two Greek soils: effects of Cs initial concentration, clay mineralogy, and particle-size fraction. Soil Sediment Contam 21(8):937–950. https://doi.org/10.1080/15320383.2012.714418

Girods P, Dufour A, Fierro V, Rogaume Y, Rogaume C, Zoulalian A, Celzard A (2009) Activated carbons prepared from wood particleboard wastes: characterisation and phenol adsorption capacities. J Hazard Mater 166(1):491–501. https://doi.org/10.1016/j.jhazmat.2008.11.047

Gouda MM, Dawood YH, Zaki AA, Salam HA, El-Naggar IMR, Gad A (2019) Adsorption characteristic of $Cs^{+}$ and $Co^{2+}$ ions from aqueous solutions onto geological sediments of radioactive waste disposal site. J Geochem Explor 206:106366. https://doi.org/10.1016/j.gexplo.2019.106366

Greenwood NN, Earnshaw A (1997) Chemistry of the elements. Butterworth-Heinemann Publication, Oxford. https://doi.org/10.1016/C2009-0-30414-6

Gülten A, Tuba S (1996) Adsorption of 4,4' - iso propylidene diphenol and diphenylolpropane 4,4' dioxyaceticacid from aqueous solution on kaolinite. J Environ Sci Health Part a: Environ Sci Eng Toxic 31(8):2055–2069. https://doi.org/10.1080/10934529609376474

Haghseresht CF, Lu GQ (1998) Adsorption characteristics of phenolic compounds onto coal-reject-derived adsorbents. Energy Fuels 12(6):1100–1107. https://doi.org/10.1021/ef9801165

Hamed MM, Aly MI, Nayl AA (2016) Kinetics and thermodynamics studies of cobalt, strontium and caesium sorption on marble from aqueous solution. Chem Ecol 32(1):68–87. https://doi.org/10.1080/02757540.2015.1112379

Hassan HB (2016) Effect of Suez canal marine sediment on sorption of cesium. J Nuc Technol Appl Sci 4(3):113–121

Ho YS, McKay G (1999) Pseudo-second order model for sorption processes. Process Biochem 34(5):451–465. https://doi.org/10.1016/S0032-9592(98)00112-5

Huitti T, Hakanen M, Lindberg A (2000) Sorption and desorption of cesium on rapakivi granite and its minerals. Working Report, Posiva Oy, Helsinki, Finland. https://inis.iaea.org/collection/NCLCollectionStore/_Public/31/042/31042251.pdf

Hwang J, Choung S, Shin W, Han WS, Chon CM (2021) A batch experiment of Cesium uptake using illitic clays with different degrees of crystallinity. Water 13(4):409. https://doi.org/10.3390/w13040409

Inzoli S (2016) Experimental and statistical methods to improve the reliability of spectral induced polarization to infer litho-textural properties of alluvial sediments. PhD thesis, Università degli studi di Milano. https://doi.org/10.13130/inzoli-silvia_phd2016-02-10

ISO (International Organization for Standardization). Determination of the specific surface area of solids by gas adsorption — BET method. ISO Standard No. 9277:2022. https://www.iso.org/standard/71014.html

Latrille C, Bildstein O (2022) Cs selectivity and adsorption reversibility on Ca-illite and Ca-vermiculite. Chemosphere. https://doi.org/10.1016/j.chemosphere.2021.132582

Lee J, Park SM, Jeon EK, Baek K (2017) Selective and irreversible adsorption mechanism of cesium on illite. Appl Geochem 85:188–193. https://doi.org/10.1016/j.apgeochem.2017.05.019

Lee WE, Ojovan MI, Jantzen CM (2013) Radioactive waste management and contaminated site clean-up: processes technologies and international experience. Woodhead Publishing, Hardback

Lemieux P, Lee S, Mikelonis A, Boe T, Hudson S (2018) Summary of the Transport of Cesium in the Environment. U.S. Environmental Protection Agency, Washington, DC, EPA/600/S-18/289. https://cfpub.epa.gov/si/si_public_file_download.cfm?p_download_id=537016&Lab=NHSRC

Li X, Tang L, Liu N, Chang Q, Zhang J (2021) Coupling of adsorption site and cation ratio regulates the adsorption of $Cs^+$ and $Na^+$ at the surface of clay mineral. Appl Clay Sci. https://doi.org/10.1016/j.clay.2021.106121d

Li Y, Du Q, Wang X, Zhang P, Wang D, Wang Z, Xia Y (2010) Removal of lead from aqueous solution by activated carbon prepared from Enteromorpha prolifera by zinc chloride activation. J Hazard Mater 183(1–3):583–589. https://doi.org/10.1016/j.jhazmat.2010.07.063

Malash GF, El-Khaiary MI (2010) Piecewise linear regression: a statistical method for the analysis of experimental adsorption data by the intraparticle-diffusion models. Chem Eng J 163(3):256–263. https://doi.org/10.1016/j.cej.2010.07.059

McKinley JP, Zachara JM, Heald SM, Dohnalkova A, Newville MG, Sutton SR (2004) Microscale distribution of cesium sorbed to biotite and muscovite. Environ Sci Technol 38(4):1017–1023. https://doi.org/10.1021/es034569m

Meunier A (2005) Clays. Springer, Berlin. https://doi.org/10.1007/b138672

Missana T, Benedicto A, García-Gutiérrez M, Alonso U (2014a) Modeling cesium retention onto Na-, K- and Ca-smectite: Effects of ionic strength, exchange and competing cations on the determination of selectivity coefficients. Geochim Cosmochim Acta 128:266–277. https://doi.org/10.1016/j.gca.2013.10.007

Missana T, García-Gutiérrez M, Benedicto A, Ayora C, De-Pourcq K (2014b) Modelling of Cs sorption in natural mixed-clays and the effects of ion competition. Appl Geochem 49:95–102. https://doi.org/10.1016/j.apgeochem.2014.06.011

Nakanishi TM, Kobayashi NI, Tanoi K (2013) Radioactive cesium deposition on rice, wheat, peach tree and soil after nuclear accident in Fukushima. J Radioanal Nucl Chem 296:985–989. https://doi.org/10.1007/s10967-012-2154-7

Okumura M, Kerisit S, Bourg IC et al (2019) Radiocesium interaction with clay minerals: theory and simulation advances Post-Fukushima. J Environ Radioact 210:105809. https://doi.org/10.1016/j.jenvrad.2018.03.011

Park S-M, Yang J-S, Tsang DCW, Alessi DS, Baek K (2019) Enhanced irreversible fixation of cesium by wetting and drying cycles in soil. Environ Geochem Health 41:149–157. https://doi.org/10.1007/s10653-018-0174-0

Reynolds WD, Gillham RW, Cherry JA (1982) Evaluation of distribution coefficients for the prediction of strontium and cesium migration in a uniform sand. Can Geotech J 19(1):92–103. https://doi.org/10.1139/t82-008

Rudzinski W, Plazinski W (2006) Kinetics of solute adsorption at solid/solution interfaces: a theoretical development of the empirical pseudo-first and pseudo-second order kinetic rate equations, based on applying the statistical rate theory of interfacial transport. J Phys Chem B 110(33):16514–16525. https://doi.org/10.1021/jp061779n

Semenkova AS, Evsiunina MV, Verma PK, Mohapatra PK, Petrov VG, Seregina IF, Bolshov MA, Krupskaya VV, Romanchuk AY, Kalmykov SN (2018) $Cs^+$ sorption onto Kutch clays: Influence of competing ions. Appl Clay Sci 166:88–93. https://doi.org/10.1016/j.clay.2018.09.010

Shahwan T, Erten HN (2002) Thermodynamic parameters of $Cs^+$ sorption on natural clays. J Radioanal Nucl Chem 253:115–120. https://doi.org/10.1023/A:1015824819940

Shenber MA, Eriksson A (1993) Sorption behaviour of caesium in various soils. J Environ Radioact 19(1):41–51

Sheppard MI, Thibault DH (1990) Default soil solid/liquid partition coefficients Kd, for four major soil types: a compendium. Health Phys 59(4):471–482

Staunton S, Roubaud M (1997) Adsorption of $^{137}Cs$ on montmorillonite and illite: effect of charge compensating cation, ionic strength, concentration of Cs, K and fulvic acid. Clays Clay Miner 45(2):251–260. https://doi.org/10.1346/CCMN.1997.0450213

Steinhauser G, Brandl A, Johnson TE (2014) Comparison of the Chernobyl and Fukushima nuclear accidents: a review of the environmental impacts. Sci Total Environ 470–471:800–817. https://doi.org/10.1016/j.scitotenv.2013.10.029

Szabo J (2018) Persistence and decontamination of radioactive cesium-137 in a model drinking water system. U.S. Environmental Protection Agency, Washington, DC, EPA/600/R-18/017. https://cfpub.epa.gov/si/si_public_record_report.cfm?dirEntryId=341673

Tachi Y, Sato T, Takeda C, Ishidera T, Fujiwara K, Iijima K (2020) Key factors controlling radiocesium sorption and fixation in river sediments around the Fukushima Daiichi nuclear power plant. Part 2: sorption and fixation behaviors and their relationship to sediment properties. Sci Total Environ 724:138097. https://doi.org/10.1016/j.scitotenv.2020.138097

Tanaka T, Ohnuki T (1994) Influence of soil/solution ratio on adsorption behavior of cesium on soils. Geochem J 28(5):369–376. https://doi.org/10.2343/geochemj.28.369

Testoni R, Levizzari R, De Salve M (2017) Analysis on distribution coefficient of Strontium and cesium for safety assessment studies. J Radioanal Nucl Chem 312:305–316. https://doi.org/10.1007/s10967-017-5224-z

Toby BH, Von Dreele RB (2013) GSAS-II: the genesis of a modern open-source all purpose crystallography software package. J Appl Crystallogr 46(2):544–549. https://doi.org/10.1107/S0021889813003531

Torstenfelt B, Andersson K, Allard B (1982) Sorption of strontium and cesium on rocks and minerals. Chem Geol 36:123–137. https://doi.org/10.1016/0009-2541(82)90042-0

Toshiaki O (1984) Ion exchange adsorption of radioactive cesium, cobalt, manganese, and strontium to granitoid rocks in the presence of competing cations. Nucl Technol 67(1):92–101. https://doi.org/10.13182/NT84-A33532

Tsuji T, Matsumura D, Kobayashi T, Suzuki S, Yoshii K, Nishihata Y, Yaita T (2014) Local structure around cesium in montmorillonite, vermiculite and zeolite under wet condition. Clay Sci 18(4):93–97. https://doi.org/10.11362/jcssjclayscience.18.4_93

Ueda S, Hasegawa H, Kakiuchi H, Akata N, Ohtsuka Y, Hisamatsu S (2012) Fluvial discharges of Radiocaesium from watersheds contaminated by the Fukushima Dai-ichi nuclear power plant accident, Japan. J Environ Radioact 118:96–104. https://doi.org/10.1016/j.jenvrad.2012.11.009

Ugur FA, Sahan H (2012) Sorption behaviour of 137Cs on Kaolinite. Ekoloji 21(82):34–40. https://doi.org/10.5053/ekoloji.2011.825

Wang T-H, Li M-H, Wei Y-Y, Teng S-P (2010) Desorption of cesium from granite under various aqueous conditions. Appl Radiat Isot 68(12):2140–2146. https://doi.org/10.1016/j.apradiso.2010.07.005

Weber WJ, Morris JC (1963) Kinetics of adsorption on carbon from solution. J Sanit Eng Division 89(2):31–60. https://doi.org/10.1061/JSEDAI.0000430

Whitney D, Evans B (2010) Abbreviations for names of rock-forming minerals. Am Miner 95(1):185–187. https://doi.org/10.2138/am.2010.3371

Yasunari TJ, Stohl A, Hayano RS, Burkhart JF, Eckhardt S, Yasunari T (2011) Cesium-137 deposition and contamination of Japanese

soils due to the Fukushima nuclear accident. Proc Natl Acad Sci USA (PNAS) 108(49):19530–19534. https://doi.org/10.1073/pnas.1112058108

Yildiz B, Erten HN, Kis M (2011) The sorption behavior of $Cs^+$ ion on clay minerals and zeolite in radioactive waste management: sorption kinetics and thermodynamics. J Radioanal Nucl Chem 288:475–483. https://doi.org/10.1007/s10967-011-0990-5

Yin X, Wang X, Wu H, Ohnuki T, Takeshita K (2017) Enhanced desorption of cesium from collapsed interlayer regions in vermiculite by hydrothermal treatment with divalent cations. J Hazar Mater 326:47–53. https://doi.org/10.1016/j.jhazmat.2016.12.017

Yoshida S, Muramatsu Y, Dvornik AM, Zhuchenko TA, Linkov I (2004) Equilibrium of radiocesium with stable caesium within biological cycle of contaminated forest ecosystems. J Environ Radioact 75(3):301–313. https://doi.org/10.1016/j.jenvrad.2003.12.008

Zachara JM, Smith SC, Liu C, McKinley JP, Serne RJ, Gassman PL (2002) Sorption of $Cs^+$ to micaceous subsurface sediments from the Hanford site, USA. Geochim Cosmochim Acta 66(2):193–211. https://doi.org/10.1016/S0016-7037(01)00759-1

Zhang K, Li Z, Qi S, Chen W, Xie J, Wu H, Zhao H, Li D, Wang S (2022) Adsorption behavior of Cs(I) on natural soils: Batch experiments and model-based quantification of different adsorption sites. Chemosphere. https://doi.org/10.1016/j.chemosphere.2021.132636

Zhu YG, Smolders E (2000) Plant uptake of radiocaesium: a review of mechanisms, regulation, and application. J Exp Bot 51(351):1635–1645. https://doi.org/10.1093/jexbot/51.351.1635